

Supporting Information

Inorganic–organic-hybrid Cu–dipyridyl semiconducting polymers based on redox-active cluster $[\text{SFe}_3(\text{CO})_9]^{2-}$: filling the gap in iron carbonyl chalcogenide polymers

Ming-Chi Hsu,^a Ru Yan Lin,^a Tzu-Yen Sun,^a Yu-Xin Huang,^a Min-Sian Li,^a Yu-Huei Li,^a
Hui-Lung Chen^{*b} and Minghuey Shieh^{*a}

^a Department of Chemistry, National Taiwan Normal University, Taipei, Taiwan 116325,
Republic of China

^b Department of Chemistry and Institute of Applied Chemistry, Chinese Culture University,
Taipei 111396, Taiwan, Republic of China

*To whom all correspondence should be addressed. E-mail: mshieh@ntnu.edu.tw (M. Shieh);
chl3@faculty.pccu.edu.tw (H.-L. Chen)

Contents

| | |
|---|-------|
| Other experimental details | 1–4 |
| Explanation for Checkcif alert of polymer 1-dpy-2D | 5 |
| Fig. S1 PXRD patterns of 1-bpea-1D and 1-bpee-1D via three-component LAG synthesis. | 6 |
| Fig. S2 PXRD patterns of transformations between 1-bpea-1D and 1-bpea-2D . | 7 |
| Fig. S3 PXRD patterns of transformations between 1-bpee-2D-1 and 1-bpee-2D-3·MeCN . | 8 |
| Fig. S4 PXRD patterns of transformations from 1-bpee-2D-2 to 1-bpee-2D-1 and to 1-bpee-2D-3·MeCN . | 9 |
| Fig. S5 ORTEP diagrams of 1-bpea-2D , 1-bpee-2D-1·MeCN , 1-bpee-2D-2 , 1-bpee-2D-3·MeCN , 1-dpy-2D , and 1-dpy-1D . | 10–12 |
| Fig. S6 PXRD patterns of 1-dpy-2D , 1-dpy-1D , and 1-bpp-2D via three-component LAG synthesis. | 13–14 |
| Fig. S7 Portions of polymeric frameworks of 1-dpy-2D and 1-dpy-1D . | 15 |
| Fig. S8 Portions of the five-fold interpenetrated framework in polymer 1-dpy-2D . | 16 |
| Fig. S9 PXRD patterns of transformations between 1-dpy-2D and 1-dpy-1D . | 17 |
| Fig. S10 Topology analysis of 1-bpea-2D , 1-bpee-2D-1·MeCN , 1-bpee-2D-2 , 1-bpee-2D-3·MeCN , and 1-dpy-2D . | 18–19 |
| Fig. S11 Packing diagrams of 1-bpea-2D , 1-bpee-2D-1·MeCN , 1-bpee-2D-2 , 1-bpee-2D-3·MeCN , 1-dpy-1D , and 1-dpy-2D . | 20–22 |
| Fig. S12 TGA spectra of the resultant polymers. | 23–24 |
| Fig. S13 Diffuse reflectance spectra of the resultant polymers. | 25–26 |
| Fig. S14 <i>I-V</i> curves for pressed pellets of the resultant polymers. | 27–28 |

| | |
|--|-------|
| Fig. S15 XPS spectra of the resultant polymers. | 29–30 |
| Fig. S16 XANES spectra of the resultant polymers. | 31–32 |
| Fig. S17 DOS plots of 1-bpee-1D , 1-bpea-2D , 1-bpee-2D-1·MeCN , 1-bpee-2D-2 , 1-bpee-2D-3·MeCN , 1-dpy-2D , 1-dpy-1D , and 1-bpp-2D . | 33–34 |
| Fig. S18 The pCOHP plots of selected Cu–N, Cu–S, Cu–Fe, and Cu–Cu bonds. | 35–36 |
| Fig. S19 Calculated band structures of 1-bpee-1D , 1-bpea-2D , 1-bpee-2D-1·MeCN , 1-bpee-2D-2 , 1-bpee-2D-3·MeCN , 1-dpy-2D , 1-dpy-1D , and 1-bpp-2D . | 37–38 |
| Fig. S20 DPVs of 1-bpea-2D , 1-bpee-1D , 1-bpee-2D-3·MeCN , 1-bpee-2D-1 , and 1-dpy-1D . | 39 |
| Table S1 Selected crystallographic data for 1-bpea-2D , 1-bpee-2D-1·MeCN , 1-bpee-2D-2 , 1-bpee-2D-3·MeCN , 1-dpy-2D , and 1-dpy-1D . | 40–41 |
| Table S2 Selected bond distances (Å) and bond angles (deg) for 1-bpea-2D , 1-bpee-2D-1·MeCN , 1-bpee-2D-2 , 1-bpee-2D-3·MeCN , 1-dpy-2D , and 1-dpy-1D . | 42–46 |
| Table S3 Detailed investigation of TGA spectra. | 47 |
| Table S4 Contributions (%) in PDOS for valence and conduction bands. | 48 |
| References | 49 |

Other experimental details

Synthesis of $[(\mu_3\text{-S})\text{Fe}_3(\text{CO})_9\text{Cu}_2(\text{bpea})]_n$ (1-bpea-1D**).** A powder mixture of $[\text{Et}_4\text{N}]_2[\mathbf{1}]$ (199 mg, 0.28 mmol), $[\text{Cu}(\text{MeCN})_4][\text{BF}_4]$ (177 mg, 0.56 mmol), and bpea (52 mg, 0.28 mmol) was grounded with ca. 250 μL of $\text{Et}_2\text{O}/\text{THF}$ in an agate mortar until the solvent had evaporated ($v/v = 1/1$, two times, 30 min in total). The residue was washed with H_2O to give the reddish product of **1-bpea-1D** (211 mg, 0.28 mmol; $\sim 100\%$ based on $[\text{Et}_4\text{N}]_2[\mathbf{1}]$), in which the PXRD pattern matched the simulation generated from the X-ray data of $[\text{TeFe}_3(\text{CO})_9\text{Cu}_2(\text{bpea})]_n$ (Fig. S1a).¹ Elemental analysis calcd. for **1-bpea-1D**: C, 33.06; H, 1.59; N, 3.67. Found: C, 32.78; H, 1.98; N, 3.75. IR (ATR): $\nu_{\text{CO}} = 2042$ (w), 1982 (m), 1943 (sh), 1874 (br), 1856 (sh) cm^{-1} .

Synthesis of $[(\mu_3\text{-S})\text{Fe}_3(\text{CO})_9\text{Cu}_2(\text{bpee})]_n$ (1-bpee-1D**).** The process used to synthesize **1-bpea-1D** was applied to **1-bpee-1D**, in which $[\text{Et}_4\text{N}]_2[\mathbf{1}]$ (200 mg, 0.28 mmol), $[\text{Cu}(\text{MeCN})_4][\text{BF}_4]$ (177 mg, 0.56 mmol), and bpee (51 mg, 0.28 mmol) were used. This LAG reaction was grounded with ca. 500 μL of THF (two times, 40 min in total) and then washed with H_2O to give the reddish-brown product of **1-bpee-1D** (186 mg, 0.24 mmol; 87% based on $[\text{Et}_4\text{N}]_2[\mathbf{1}]$), in which the PXRD pattern matched the simulation generated from the X-ray data of $[(\text{TeFe}_3(\text{CO})_9\text{Cu}_2(\text{bpee}))]_n$ (Fig. S1b).¹ Elemental analysis calcd. for **1-bpee-1D**: C, 33.50; H, 1.72; N, 3.63. Found: C, 33.14; H, 1.32; N, 3.68. IR (ATR): $\nu_{\text{CO}} = 2041$ (w), 1988 (vs), 1949 (m), 1938 (sh), 1915 (s), 1888 (sh), 1878 (s), 1859 (s) cm^{-1} .

Synthesis of $[(\mu_4\text{-S})\text{Fe}_3(\text{CO})_9\text{Cu}_2(\text{MeCN})(\text{dpy})_{1.5}]_n$ (1-dpy-2D**).** The process used to synthesize **1-bpea-1D** was applied to **1-dpy-2D**, in which powder samples of $[\text{Et}_4\text{N}]_2[\mathbf{1}]$ (199 mg, 0.28 mmol), $[\text{Cu}(\text{MeCN})_4][\text{BF}_4]$ (177 mg, 0.56 mmol), and dpy (66 mg, 0.42 mmol) were used. This LAG reaction was ground with ca. 150 μL of MeCN and then washed with H_2O to give the reddish sample of **1-dpy-2D** (187 mg, 0.22 mmol; 79% based on $[\text{Et}_4\text{N}]_2[\mathbf{1}]$), in which the PXRD pattern matched the simulation generated from the X-ray data of **1-dpy-2D** (Fig. S6a). Elemental analysis calcd. for **1-dpy-2D**: C, 36.56; H, 1.77; N, 6.56. Found: C, 36.61; H, 1.91; N, 6.64. IR (ATR): $\nu_{\text{CO}} = 2020$ (w), 1972 (sh), 1934 (m), 1916 (m), 1907 (m), 1874 (m), 1864 (m), 1851 (s) cm^{-1} . Crystals of **1-dpy-2D** for X-ray diffraction were obtained from $\text{Et}_2\text{O}/\text{MeCN}/\text{DMF}$ at $-30\text{ }^\circ\text{C}$.

Synthesis of $[(\mu_3\text{-S})\text{Fe}_3(\text{CO})_9\text{Cu}_2(\text{dpy})_3]_n$ (1-dpy-1D**).** The process used to synthesize **1-bpea-1D** was applied to **1-dpy-1D**, in which $[\text{Et}_4\text{N}]_2[\mathbf{1}]$ (200 mg, 0.28 mmol), $[\text{Cu}(\text{MeCN})_4][\text{BF}_4]$ (177 mg, 0.56 mmol), and dpy (132 mg, 0.84 mmol) were used. This LAG reaction was grounded with ca. 500 μL of THF (two times, 30 min in total) and then washed with H_2O to give the reddish product of **1-dpy-1D** (289 mg, 0.28 mmol; $\sim 100\%$ based on $[\text{Et}_4\text{N}]_2[\mathbf{1}]$). The PXRD pattern matched the simulation generated from the X-ray data of **1-dpy-1D** (Fig. S6b). Elemental analysis calcd. for **1-dpy-1D**: C, 44.73; H, 2.31; N, 8.02. Found: C, 44.58; H, 2.57; N, 7.95. IR (ATR): $\nu_{\text{CO}} = 2013$ (vw), 1957 (vs), 1905 (w), 1887 (m), 1878 (s), 1865 (s) cm^{-1} . Crystals of **1-dpy-1D** for X-ray diffraction were obtained from $\text{MeOH}/\text{MeCN}/\text{DMF}$ at $4\text{ }^\circ\text{C}$.

Synthesis of $[(\mu_4\text{-S})\text{Fe}_3(\text{CO})_9\text{Cu}_2(\text{bpp})_2]_n$ (1-bpp-2D**).** The process used to synthesize **1-bpea-1D** was applied to **1-bpp-2D**, in which $[\text{Et}_4\text{N}]_2[\mathbf{1}]$ (199 mg, 0.28 mmol), $[\text{Cu}(\text{MeCN})_4][\text{BF}_4]$ (177 mg, 0.56 mmol), and bpp (112 mg, 0.56 mmol) were used. This LAG reaction was grounded with ca. 400 μL of MeCN (three times, 90 min in total) and then washed with H_2O to give the purple-red product **1-bpp-2D** (236 mg, 0.24 mmol; 86% based on $[\text{Et}_4\text{N}]_2[\text{SFe}_3(\text{CO})_9]$), in which the PXRD pattern matched the simulation generated from the X-ray data of $[(\text{SeFe}_3(\text{CO})_9\text{Cu}_2(\text{bpp})_2)]_n$ (Fig. S6c).² Elemental analysis calcd. for **1-bpp-2D**: C, 43.10; H, 2.89; N, 5.75. Found: C, 43.17; H, 2.99; N, 5.80. IR (ATR): $\nu_{\text{CO}} = 2012$ (w), 1943 (sh), 1919 (sh), 1904 (sh), 1861 (sh), 1839 (sh) cm^{-1} .

Conversion of 1-bpee-2D-2 to 1-bpee-2D-1. The process used to convert **1-bpea-1D** to **1-bpea-2D** was applied to the transformation of **1-bpee-2D-2** to **1-bpee-2D-1**, where **1-bpee-2D-2** (128 mg, 0.11 mmol based on $[(\mu_5\text{-S})\text{Fe}_3(\text{CO})_9\text{Cu}_2(\text{bpee})_3]$ unit), $[\text{Et}_4\text{N}]_2[\mathbf{1}]$ (40.1 mg, 0.06 mmol), and $[\text{Cu}(\text{MeCN})_4][\text{BF}_4]$ (35.6 mg, 0.11 mmol) were used. This LAG reaction was grounded with ca. 500 μL of MeCN (six times, 75 min in total) and then washed with H_2O to give reddish-brown product of **1-bpee-2D-1·MeCN** (147 mg, 0.16 mmol based on $[(\mu_5\text{-S})\text{Fe}_3(\text{CO})_9\text{Cu}_2(\text{bpee})_2]$ unit; 94%) with the consistent PXRD pattern from as-synthesized **1-bpee-2D-1·MeCN** (Fig. S4a).

Conversion of 1-bpee-2D-2 to 1-bpee-2D-3·MeCN. The process used to convert **1-bpea-1D** to **1-bpea-2D** was applied to the transformation of **1-bpee-2D-2** to **1-bpee-2D-3·MeCN**, where **1-bpee-2D-2** (135 mg, 0.12 mmol based on $[(\mu_5\text{-S})\text{Fe}_3(\text{CO})_9\text{Cu}_2(\text{bpee})_3]$ unit) and bpee (11.0 mg, 0.60 mmol) were used. This LAG reaction was grounded with ca. 500 μL of MeCN (four times, 60 min in total) to give **1-bpee-2D-3·MeCN** in quantitative yield with the consistent PXRD pattern from the X-ray data of **1-bpee-2D-3·MeCN** (Fig. S4b).

Conversion of 1-dpy-2D to 1-dpy-1D. The process used to convert **1-bpea-1D** to **1-bpea-2D** was applied to the conversion of **1-dpy-2D** to **1-dpy-1D**, where **1-dpy-2D** (130 mg, 0.15 mmol based on $[(\mu_4\text{-S})\text{Fe}_3(\text{CO})_9\text{Cu}_2(\text{MeCN})(\text{dpy})_{1.5}]$ unit) and dpy (36 mg, 0.23 mmol) were used. The LAG reaction was grounded with ca. 100 μL of THF (two times, 15 min in total) to give the reddish-brown **1-dpy-1D** (~100%), in which the PXRD pattern matched the simulation generated from the X-ray data of **1-dpy-1D** (Fig. S9a).

Conversion of 1-dpy-1D to 1-dpy-2D. The process used to convert **1-bpea-2D** to **1-bpea-1D** was applied to the conversion of **1-dpy-1D** to **1-dpy-2D**, where **1-dpy-1D** (104 mg, 0.10 mmol based on $[(\mu_3\text{-S})\text{Fe}_3(\text{CO})_9\text{Cu}_2(\text{dpy})_3]$ unit) $[\text{Et}_4\text{N}]_2[\mathbf{1}]$ (68 mg, 0.10 mmol), and $[\text{Cu}(\text{MeCN})_4][\text{BF}_4]$ (60 mg, 0.19 mmol) were used. This LAG reaction was grounded with ca. 200 μL of MeCN (two times, 50 min in total) and then washed with H_2O to give reddish-brown **1-dpy-2D** (165 mg, 0.19 mmol based on $[\text{SFe}_3(\text{CO})_9\text{Cu}_2(\text{MeCN})(\text{dpy})_{1.5}]$ unit; 95%), in which the PXRD pattern matched the simulation generated from the X-ray data of **1-dpy-2D** (Fig. S9b).

X-ray Structural Characterization of 1-dpy-2D, 1-dpy-1D, 1-bpea-2D, 1-bpee-2D-1·MeCN, 1-bpee-2D-2, and 1-bpee-2D-3·MeCN. Selected crystallographic data for **1-dpy-2D, 1-dpy-1D, 1-bpea-2D, 1-bpee-2D-1·MeCN, 1-bpee-2D-2, and 1-bpee-2D-3·MeCN** are given in Table S1. All crystals were mounted on glass fibers with epoxy cement. Data collection for **1-dpy-2D** and **1-dpy-1D** were performed on a Bruker Apex II CCD diffractometer, while **1-bpea-2D, 1-bpee-2D-1·MeCN, 1-bpee-2D-2, and 1-bpee-2D-3·MeCN** were performed on a Bruker D8 Venture diffractometer, using the graphite-monochromated MoK α radiation. An empirical absorption correction by the multi-scan method was applied to the data using SADABS.³ The structures were solved by direct methods and were refined with SHELXL-2014.⁴ For **1-bpee-2D-3**, the C=C group of bpee, C15 and C15' as well as C16 and C16' were disordered and presented in a 50: 50 ratio. For **1-bpea-2D**, Fe atoms, Fe1 and Fe1', Fe2 and Fe2', and Fe3 and Fe3', were disordered and presented in a 90: 10 ratio, and the carbonyls, C5 and C5', O5 and O5', C6 and C6', and O6 and O6', were disordered and presented in a 71: 29 ratio. The selected distances and angles for **1-dpy-2D, 1-dpy-1D, 1-bpea-2D, 1-bpee-2D-1·MeCN, 1-bpee-2D-2, and 1-bpee-2D-3·MeCN** are listed in Table S2.

Computational Details. Density functional theory (DFT) calculations reported in this study were performed via the periodic code of DMol³ 6.0 package⁵ with the general gradient approximation (GGA) plus the Perdew–Burke–Ernzerhof (PBE) functional⁶ and dispersion (DFT-D) calculations.⁷ Effective core potentials (ECP)⁸ and a DND basis set were used in the calculations. The geometries of **1-dpy-2D, 1-dpy-1D, 1-bpea-2D, 1-bpee-2D-1·MeCN, 1-bpee-2D-2, and 1-bpee-2D-3·MeCN** were taken from single-crystal X-ray diffraction data, and periodic structures of **1-bpp-2D** and **1-bpee-1D** were optimized by DMol³ calculation with PBE using TS method for DFT-D calculation. The state densities, crystal orbital Hamilton population, and band structures were performed on the whole crystal unit cell. The disordered part of **1-bpea-2D** with small occupancy was omitted to avoid wrong calculation results. The self-consistent-field calculations were performed with a convergence criterion 10⁻⁵ a.u. on the total energy. The global real space cutoff radius was 4.6 Å.

UV-visible Diffuse Reflectance Spectroscopy. The diffuse reflectance spectra of solid samples of all polymers were measured between 200–2500 nm for the 100% reflectance reference, poly(tetrafluoroethylene), by using a Varian Cary 5000 UV–vis–NIR spectrophotometer and the room temperature optical absorption spectra of those solid compounds were obtained from diffuse reflectance experiment. The reflectance spectrum was converted to absorption using the Kubelka-Munk function, $F = (1 - R)^2/2R$.⁹ The energy gap was determined in the F-versus-E plot by extrapolating the linear portion of the starting rising curve to zero, which provided the onset of absorption.

X-ray Photoelectron Spectroscopy. High-resolution X-ray photoelectron spectroscopy (XPS) was performed using a PHI Quantera SXM/AES 650 auger electron spectrometer (ULVAC-

PHI Inc., Japan) equipped with a monochromated Al K α ($h\nu = 1486.6$ eV) X-ray source. The samples of all polymers were deposited on a piece of conductive carbon tape, respectively. The spectra were analyzed using XPSPEAK (version 4.1) software, and the binding energy was standardized using a C 1s peak at 284.8 eV.


X-ray Absorption Near-Edge Spectroscopy. Our study recorded X-ray absorption spectra on beamlines 17C of the National Synchrotron Radiation Research Center (NSRRC) in Taiwan with a double-crystal Si(111) monochromator. The Cu K-edge spectra of all polymers were measured in transmission mode along with a reference Cu foil. Data processing and analysis were performed using the Demeter software package (version 0.9.21).¹⁰ A linear pre-edge and a linear post-edge were subtracted, and then the data were normalized by the edge height using Athena software.

Electrical Conductivity Measurements. Pressed pellets of all polymers were made by the hand-held press in the glove bag under nitrogen. A dry glass slide was used to hold the samples, and Ag paste was used to attach the two sides of the pressed pellet to the slide. The slide was then mounted onto the chuck of the probe station, and the tungsten tips were placed in the device *in vacuo*. The two-contact probe method was applied, and the I - V curve was obtained on a computer-controlled potentiostat (Jiehan, ECW-5000 electrochemical workstation) by supplying a voltage from -2 to 2 V (step size 0.05 V). The I - V curves for all samples were fitted by linear regression. A micrometer was used to measure the length (L), width (W), and thickness (T) of the samples. The electrical conductivity (σ) of all samples was calculated based on eq 1.

$$\sigma = G \times \frac{L}{A} = \frac{I}{V} \times \frac{L}{W \times T} \quad (1)$$

Solid-state Electrochemistry. The DPV measurements were recorded using a CHI 621D electrochemical potentiostat under a nitrogen atmosphere. The three-electrode system, including homemade glass carbon working electrode, platinum wire auxiliary electrode, and nonaqueous Ag/Ag⁺ electrode was used, with tetra-*n*-butylammonium perchlorate (10^{-3} M) chosen as the electrolyte and redox potentials were referred to the ferrocenium/ferrocene (Fc⁺/Fc) couple ($+0.382$ V vs MeCN, SCE). The homemade working electrode was manufactured from the grounded powdered sample (ca. 50 mg) mixed with 1.5 mL of Nafion entirely by ultrasonication for 1 minute. The resulting slurry was drop-coated onto the glassy carbon electrode to form a thin layer and dried in air for 10 minutes. Only the scan range of $-0.4 \sim +0.4$ V was analyzed due to the ease of decomposition of polymeric frameworks during the reduction process and significant interference peaks for dipyridyl ligands at $-0.8 \sim -0.6$ V. The electron stoichiometry for the DPV study was determined by analyzing the peak width at half-height ($W_{1/2}$).¹¹ Some values for the redox peaks were slightly larger than $W_{1/2} = 90$ mV, which was expected for a quasi-reversible one-electron redox reaction.¹²

Explanation for Checkcif alert of polymer 1-dpy-2D:

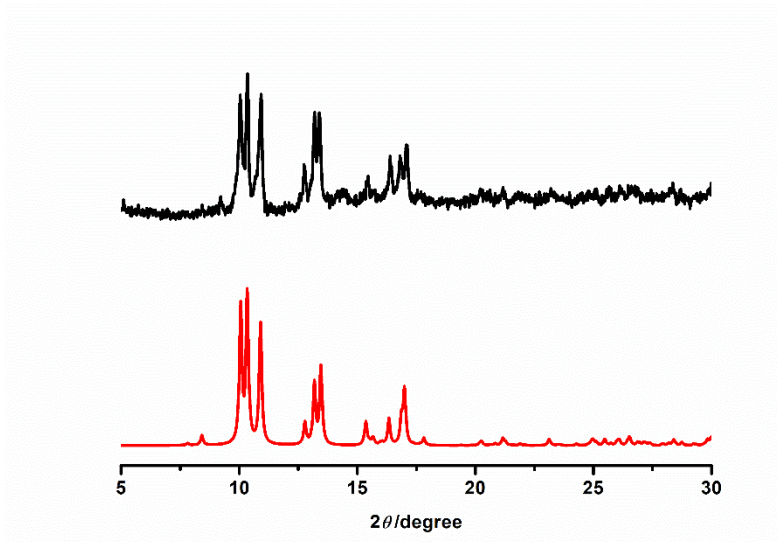
 **Alert level B**

PLAT430_ALERT_2_B Short Inter D...A Contact 05 . .05 . 2.70 Ang.
1-x, -y, 1-z = 3_656 Check

Explanation: The 2D planes of **1-dpy-2D** were closely packed which led to the short intermolecular distance between carbonyl ligands.

Fig. S1 PXRD pattern of the as-synthesized (a) **1-bpea-1D** (black line) and simulated pattern for $[\text{TeFe}_3(\text{CO})_9\text{Cu}_2(\text{bpea})]_n$ (red line) (b) **1-bpee-1D** (black line) and simulated pattern for $[\text{TeFe}_3(\text{CO})_9\text{Cu}_2(\text{bpee})]_n$ (red line).¹

(a)



(b)

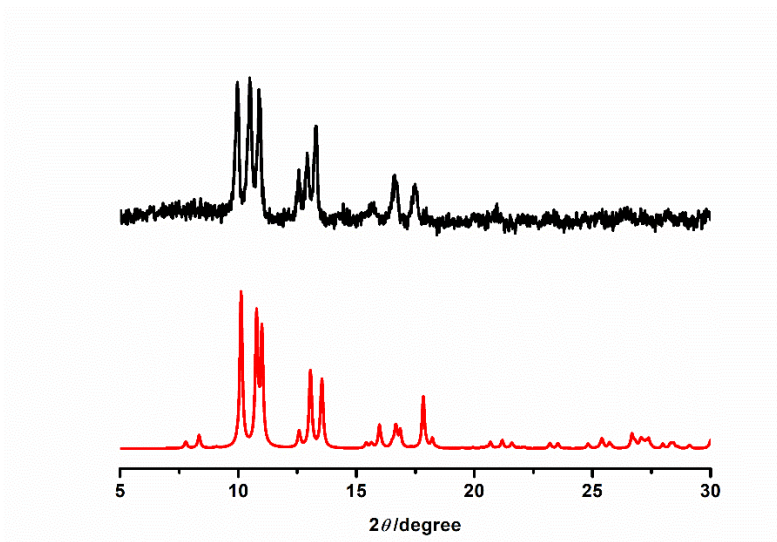


Fig. S2 PXRD patterns of the transformation of (a) **1-bpea-1D** to **1-bpea-2D** (black line) and simulated pattern for **1-bpea-2D** (red line) and (b) **1-bpea-2D** to **1-bpea-1D** (black line) and simulated pattern for $[\text{TeFe}_3(\text{CO})_9\text{Cu}_2(\text{bpea})]_n$ (red line)¹.

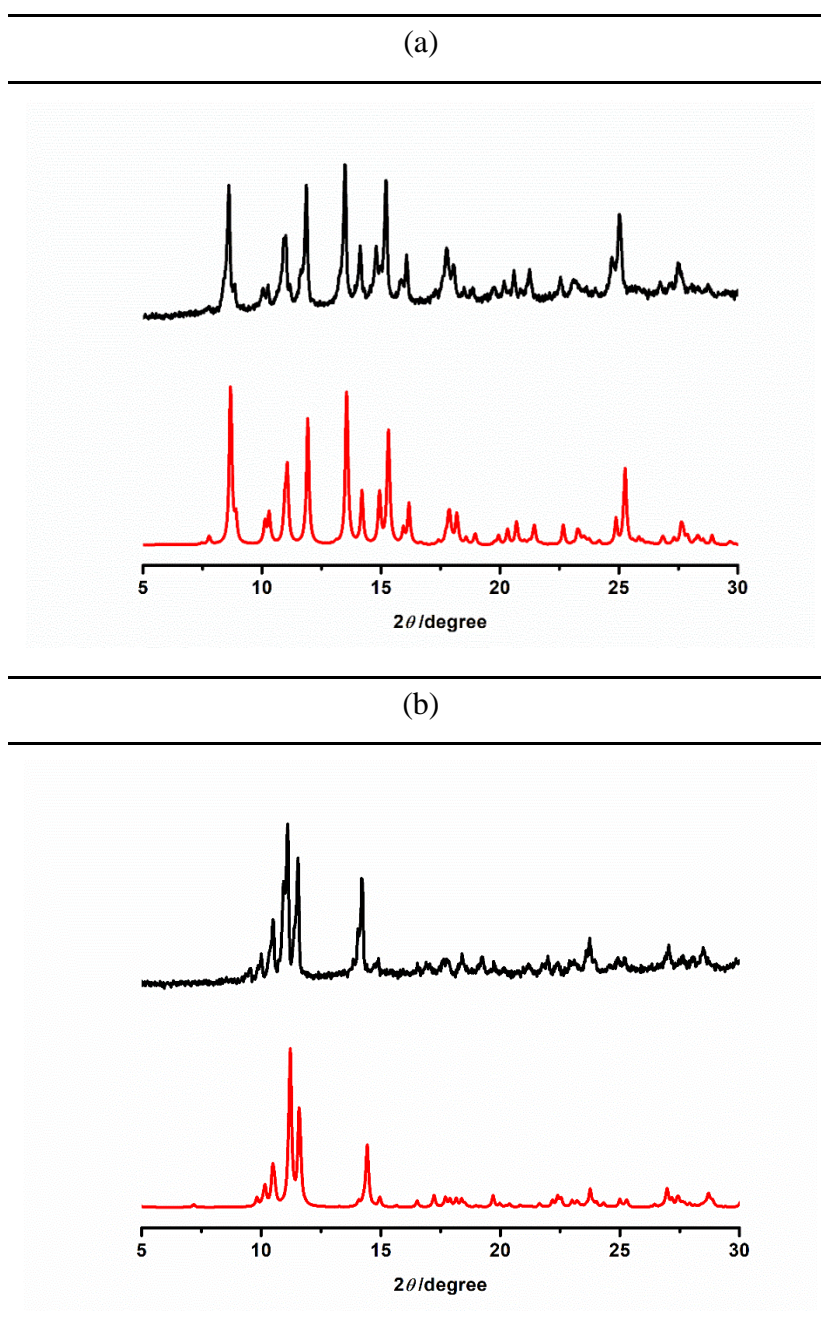
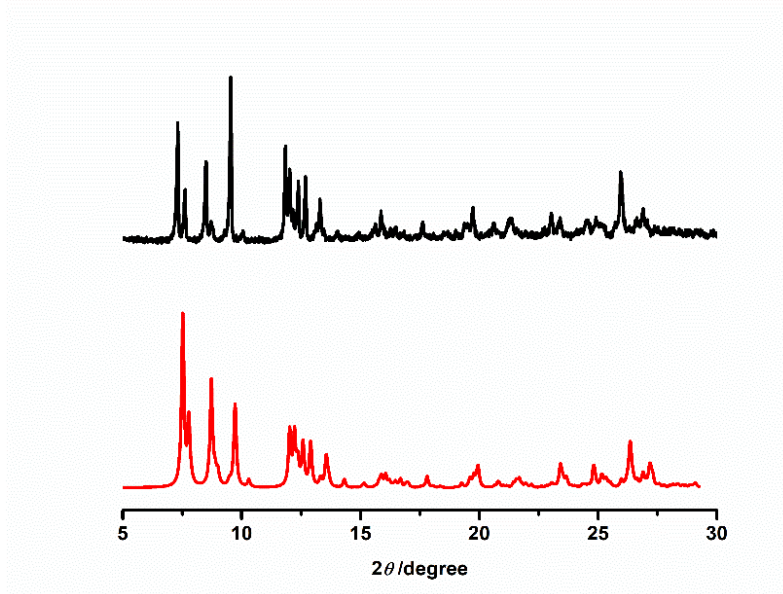


Fig. S3 PXRD patterns of the transformation of (a) **1-bpee-2D-1** to **1-bpee-2D-3·MeCN** (black line) and simulated pattern for **1-bpee-2D-3·MeCN** (red line) and (b) **1-bpee-2D-3·MeCN** to **1-bpee-2D-1** (black line) and as-synthesized pattern for **1-bpee-2D-1** (red line).

(a)



(b)

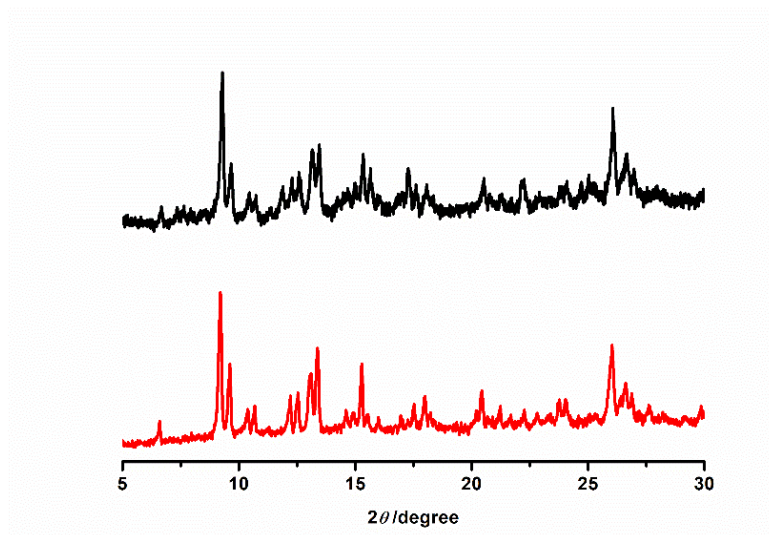
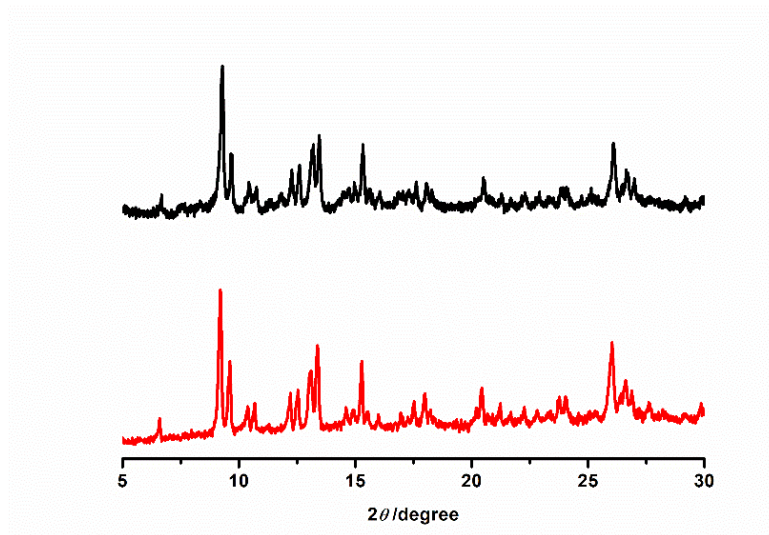


Fig. S4 PXRD patterns of the transformation of (a) **1-bpee-2D-2** to **1-bpee-2D-1** (black line) and as-synthesized pattern for **1-bpee-2D-1** (red line) and (b) **1-bpee-2D-2** to **1-bpee-2D-3·MeCN** (black line) and simulated pattern for **1-bpee-2D-3·MeCN** (red line).

(a)



(b)

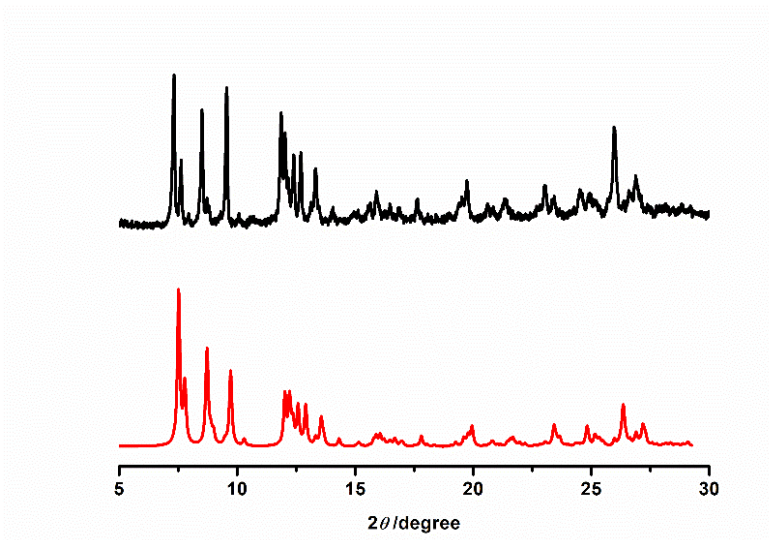
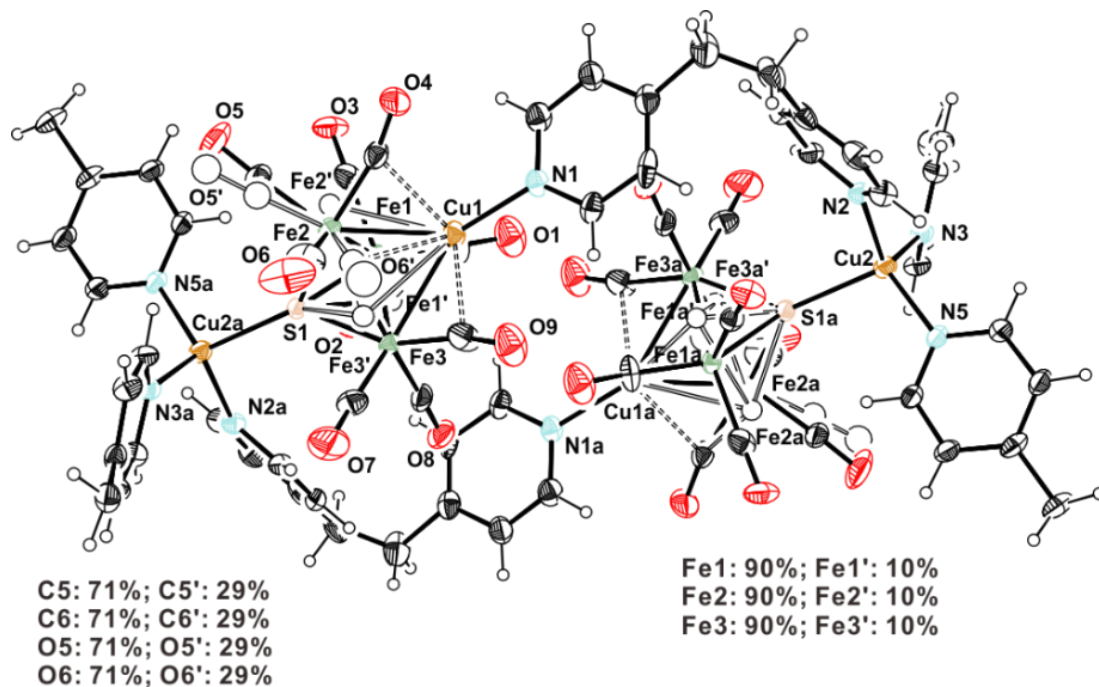
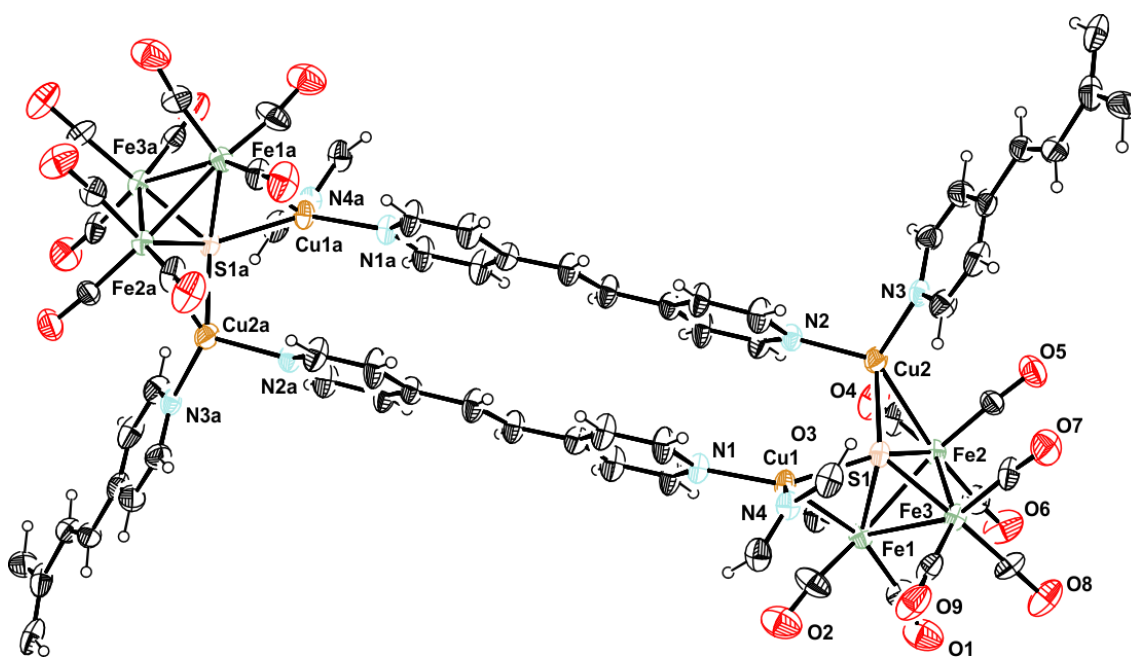


Fig. S5 ORTEP diagrams showing the structure and atom labeling for **1-bpea-2D**, **1-bpee-2D-1·MeCN**, **1-bpee-2D-2**, **1-bpee-2D-3·MeCN**, **1-dpy-2D**, and **1-dpy-1D**, (30% thermal ellipsoids). The labels for the carbon atoms are not shown for clarity.

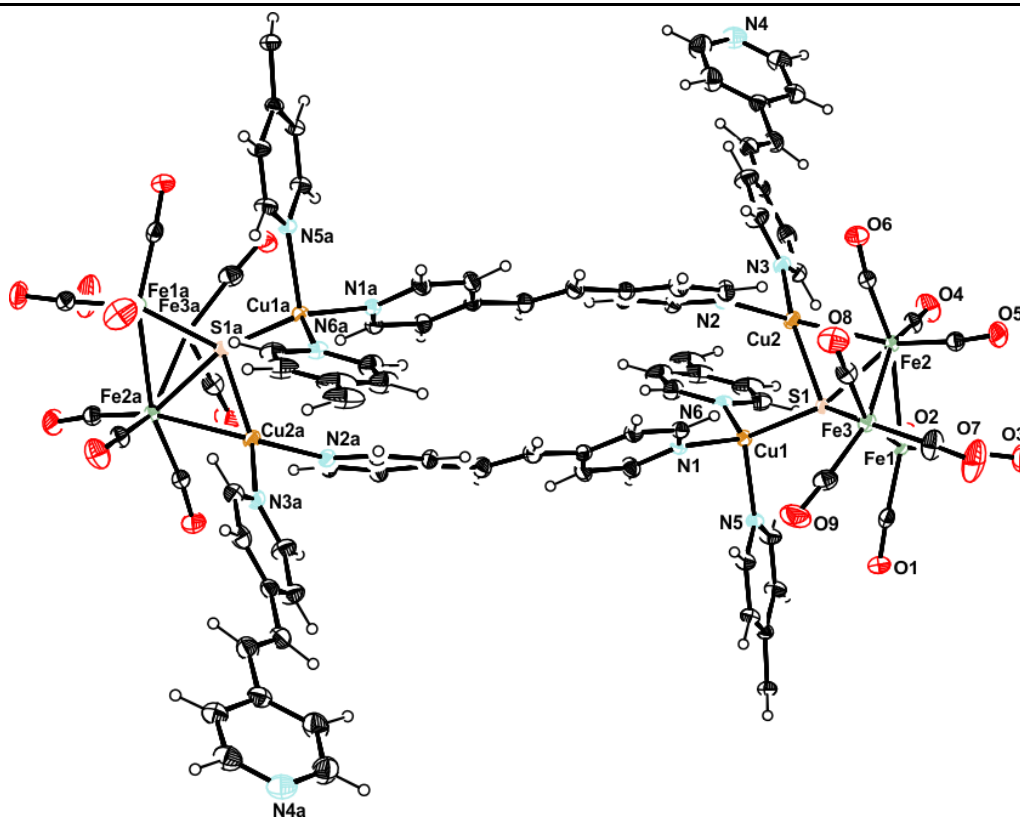
1-bpea-2D



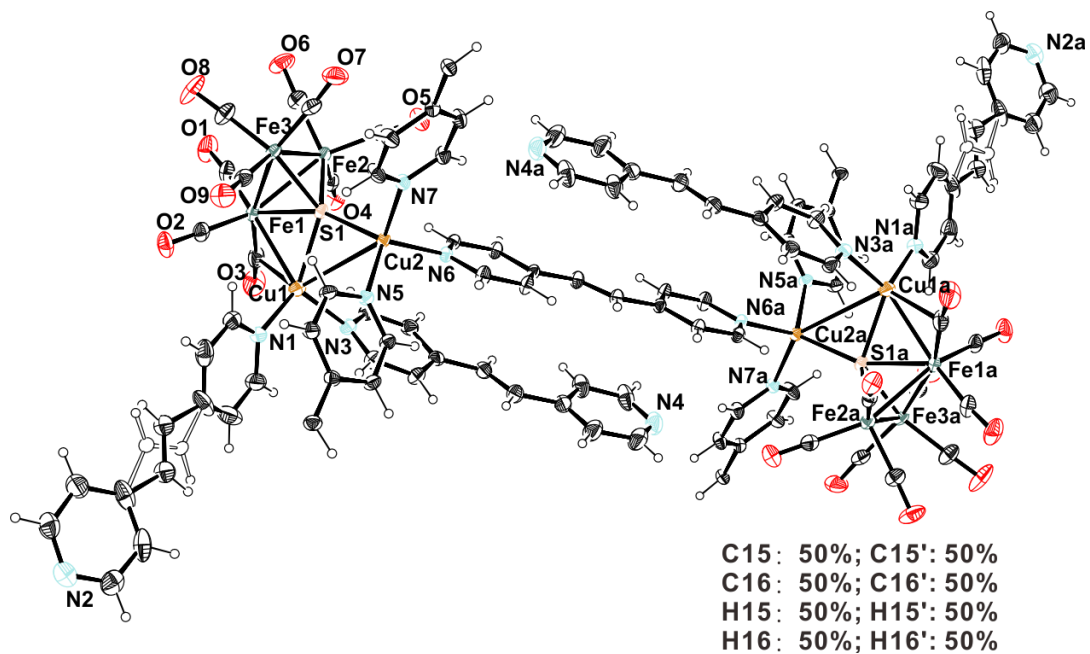
1-bpee-2D-1·MeCN (MeCN molecules were omitted)



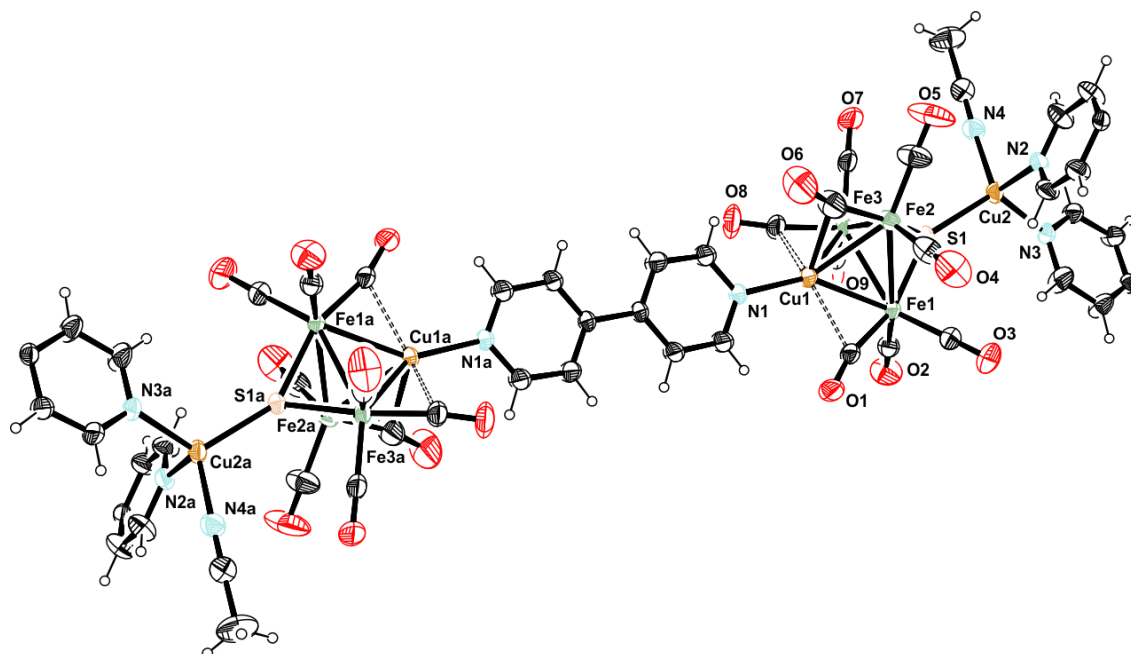
1-bpee-2D-2



1-bpee-2D-3·MeCN (MeCN molecules were omitted)



1-dpy-2D



1-dpy-1D

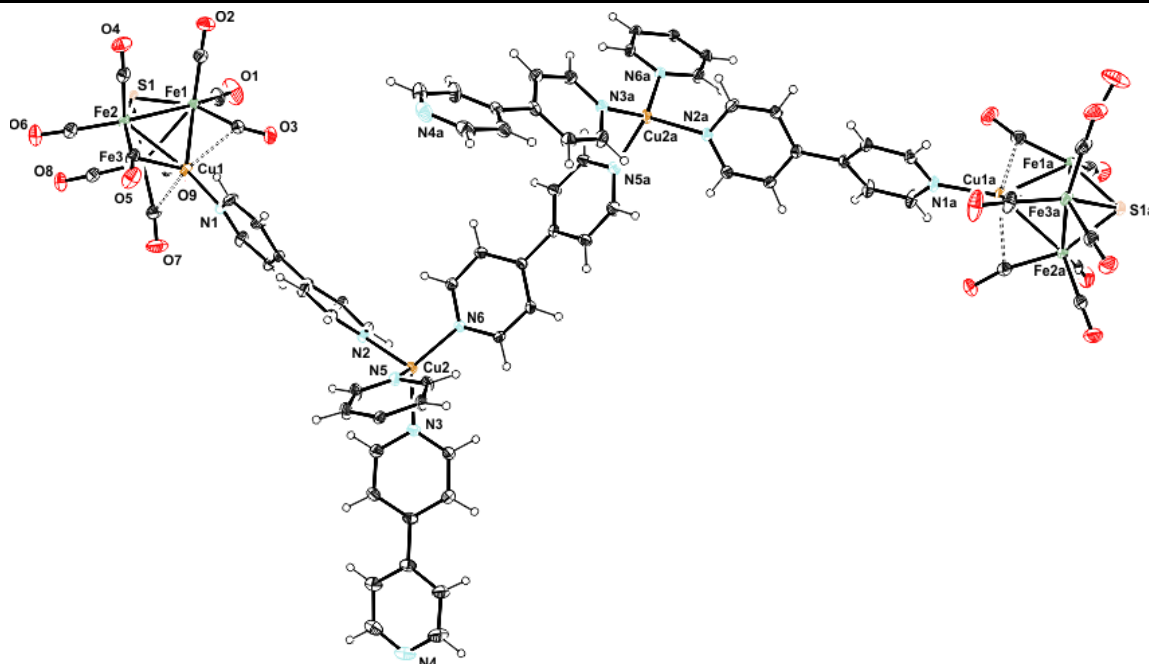
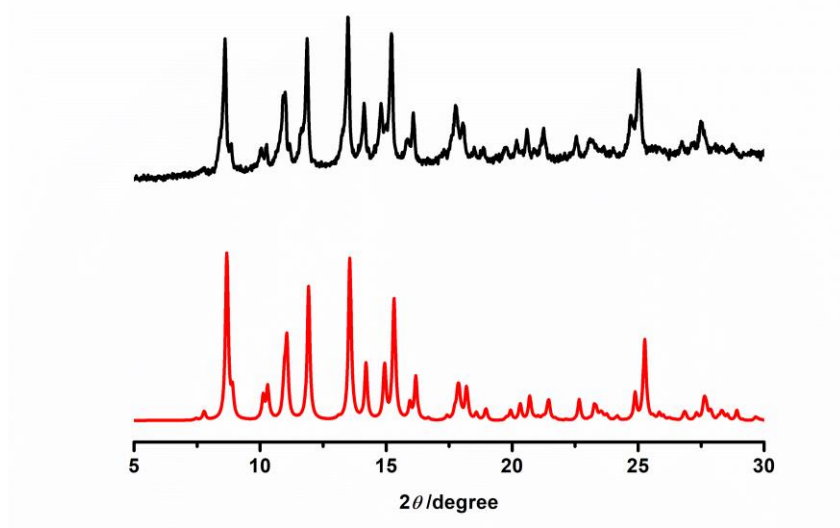
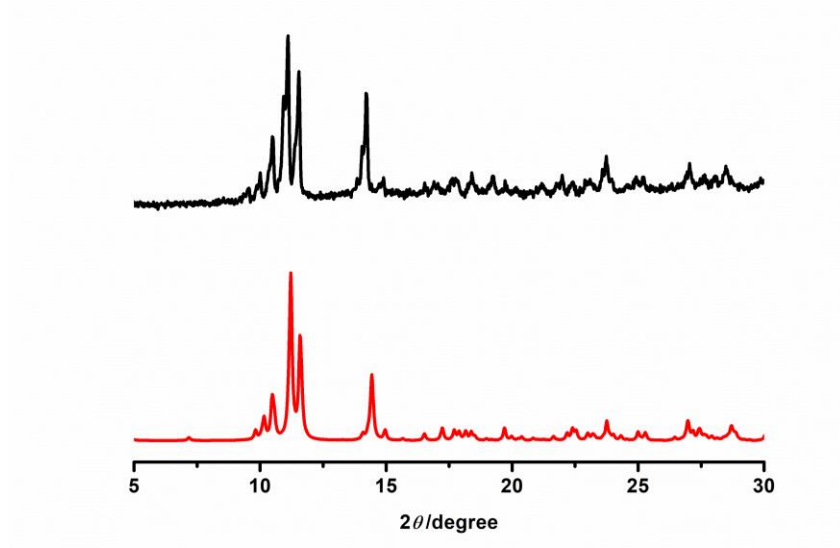


Fig. S6 PXRD pattern of the as-synthesized (a) **1-dpy-2D** (black line) and simulated pattern for **1-dpy-2D** (red line), (b) **1-dpy-1D** (black line) and simulated pattern for **1-dpy-1D** (red line), and (c) **1-bpp-2D** (black line) and simulated pattern for $[\text{SeFe}_3(\text{CO})_9\text{Cu}_2(\text{bpp})_2]_n$ (red line).²

(a)



(b)



(c)

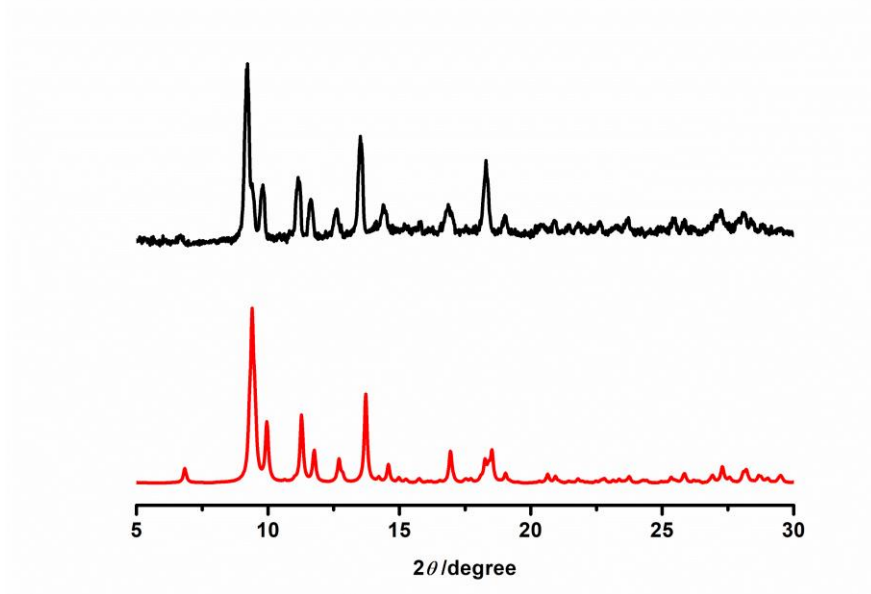
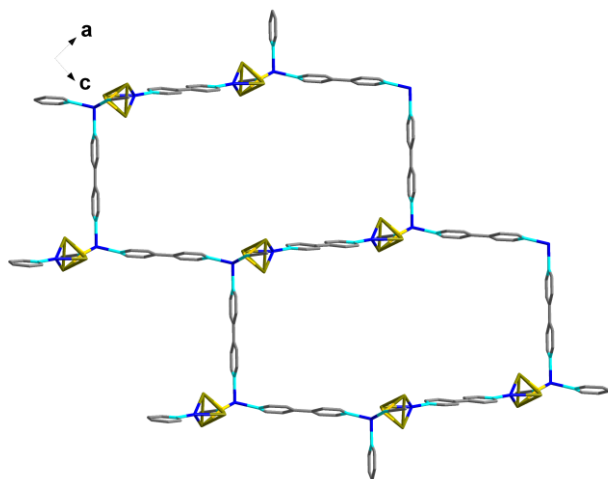


Fig. S7 Portions of polymeric frameworks of (a) **1-dpy-2D** and (b) **1-dpy-1D**. CO and H atoms were omitted for clarity.

(a)



(b)

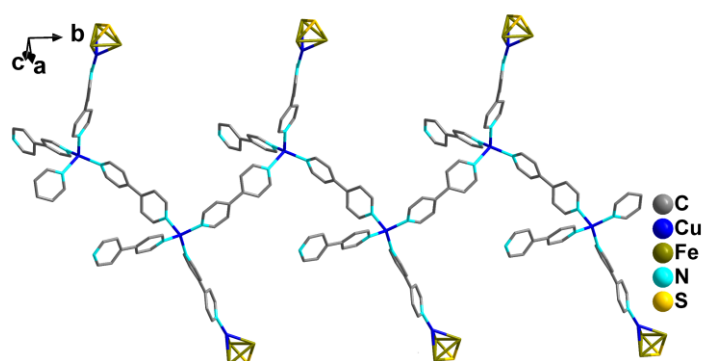


Fig. S8 The 5-fold interpenetrated 3D polymer **1-dpy-2D** in the solid-state structure. CO and H atoms were omitted for the sake of clarity.

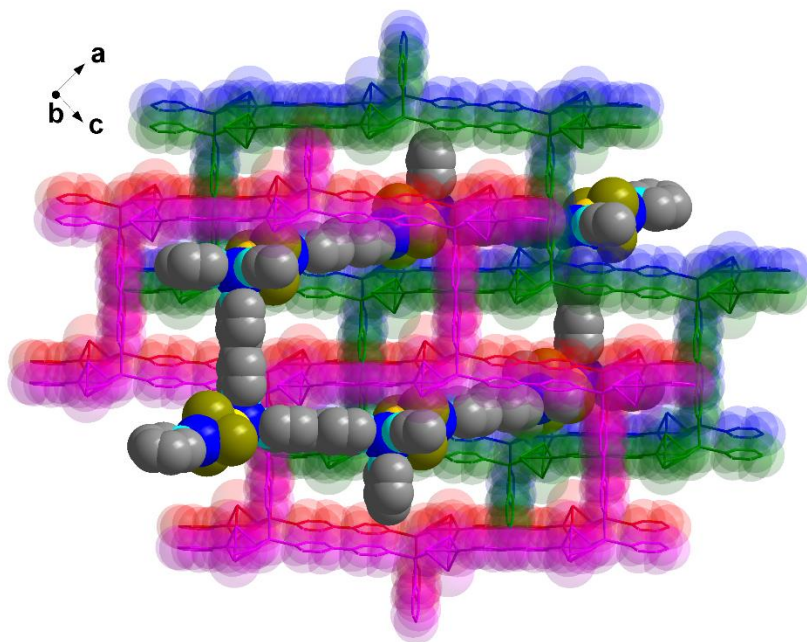


Fig. S9 Powder X-ray diffraction patterns of the transformation of (a) **1-dpy-2D** to **1-dpy-1D** (black line) and simulated pattern for **1-dpy-1D** (red line) and (b) **1-dpy-1D** to **1-dpy-2D** (black line) and simulated pattern for **1-dpy-2D** (red line).

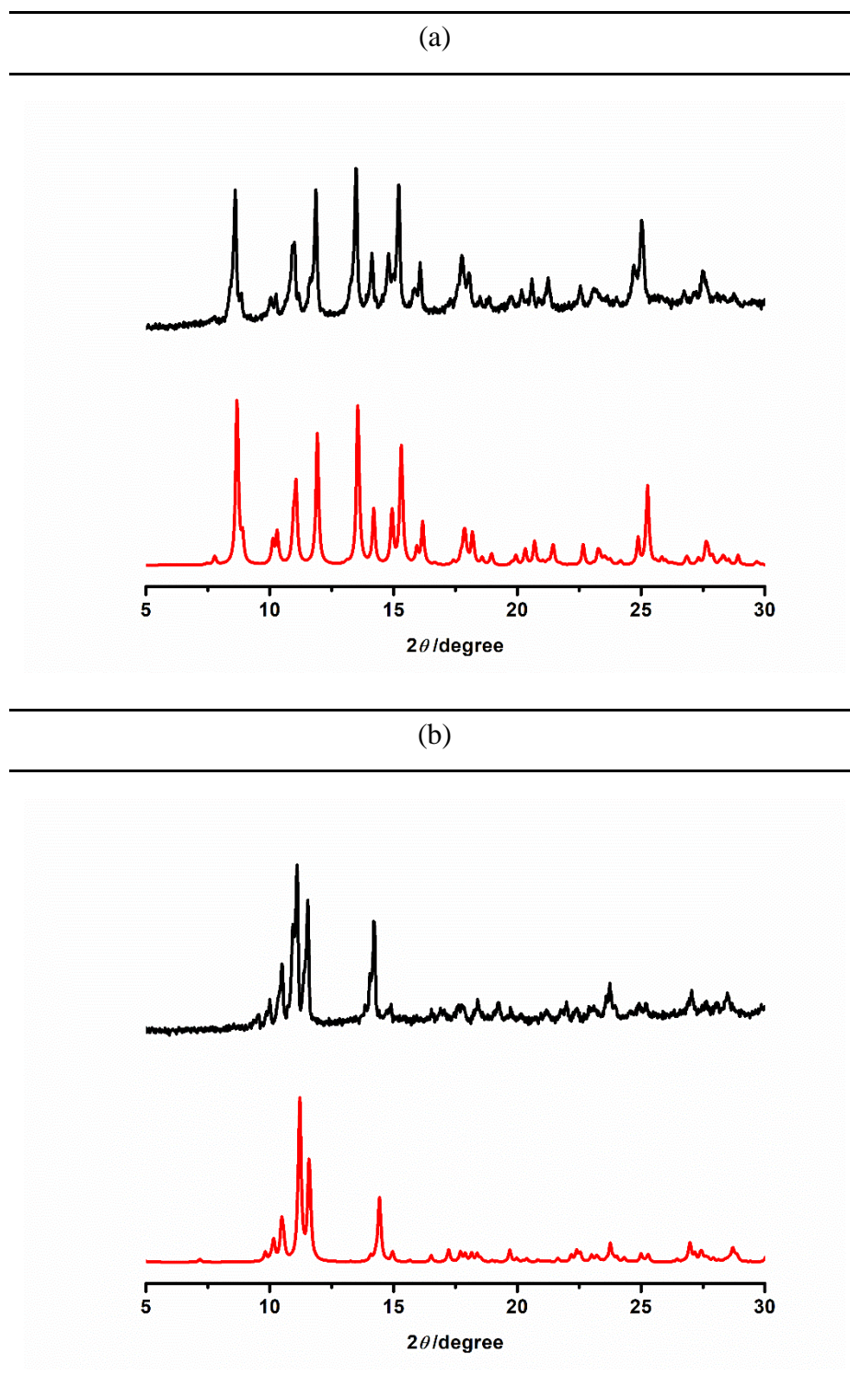
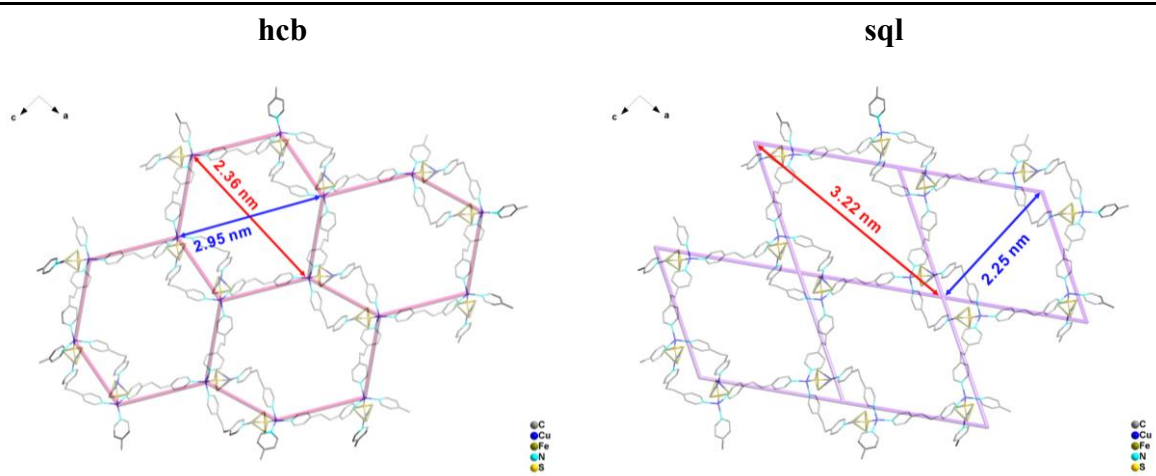
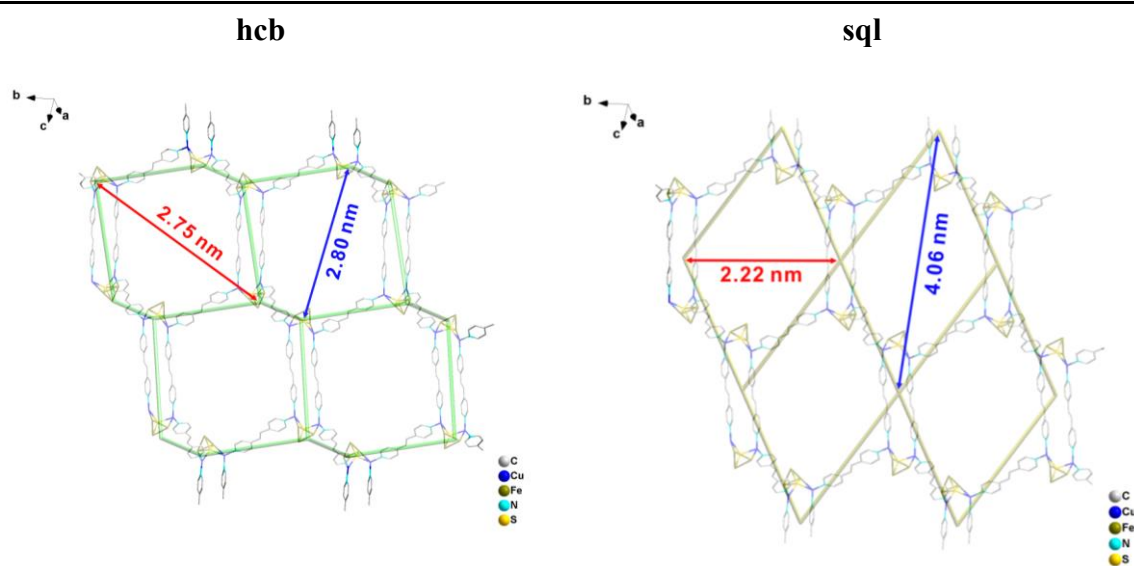


Fig. S10 Topology analysis of **1-bpea-2D**, **1-bpee-2D-1·MeCN**, **1-bpee-2D-2**, **1-bpee-2D-3·MeCN**, and **1-dpy-2D**.

1-bpea-2D

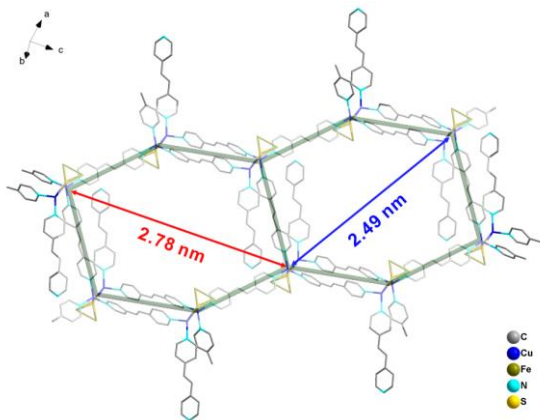


1-bpee-2D-1·MeCN

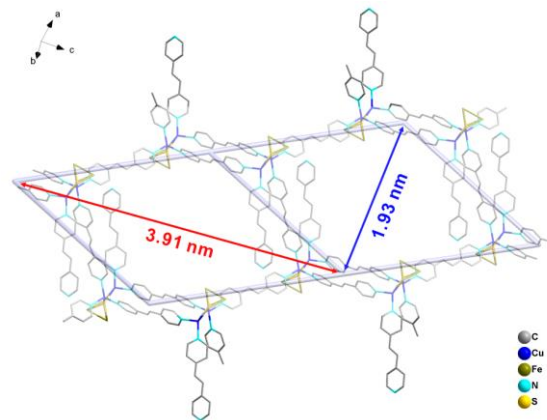


1-bpee-2D-2

hcb

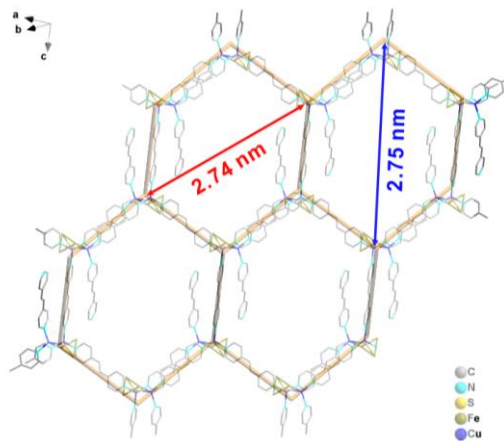


sql



1-bpee-2D-3·MeCN (disordered atoms were omitted)

hcb



1-dpy-2D

hcb

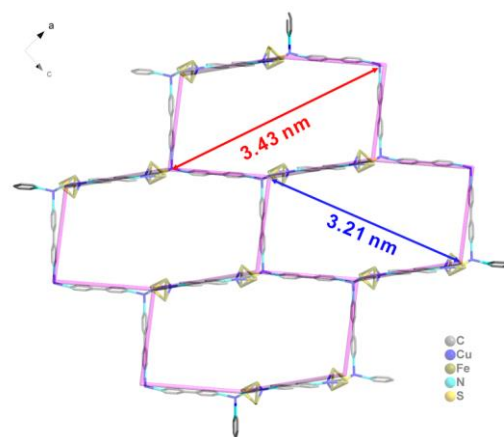
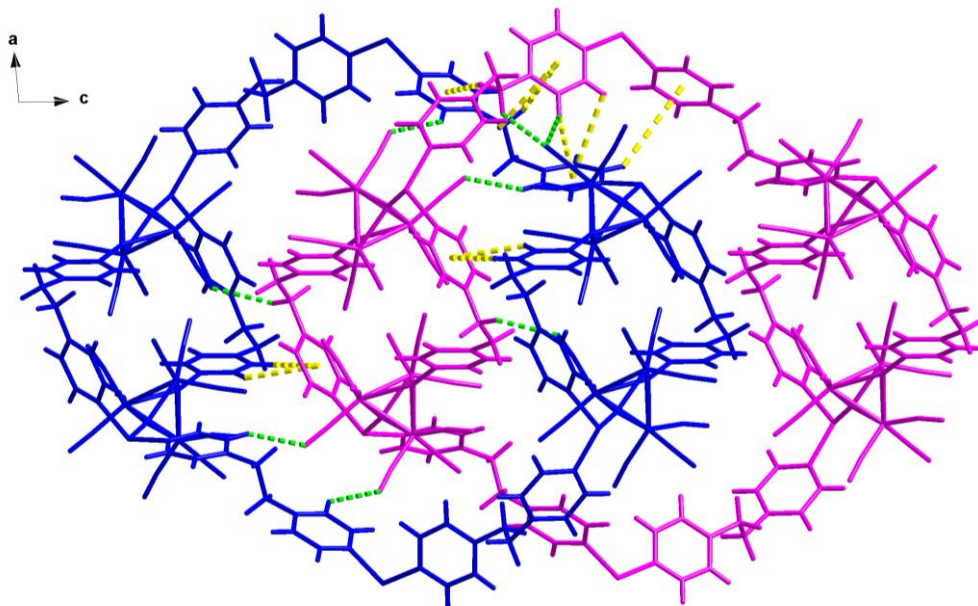
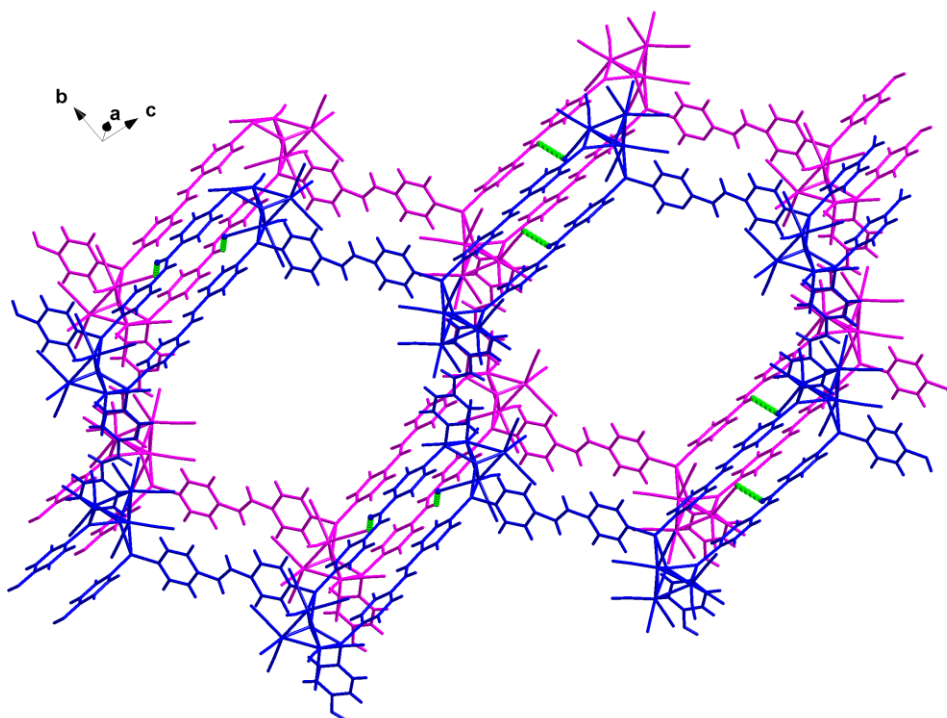


Fig. S11 Packing diagrams of **1-bpea-2D**, **1-bpee-2D-1·MeCN**, **1-bpee-2D-2**, **1-bpee-2D-3·MeCN**, **1-dpy-2D**, and **1-dpy-1D**, with broken green lines and yellow lines represented as C–H···O(carbonyl) hydrogen bonds between COs of SF₆Cu-based clusters and aromatic C–H··· π interactions.

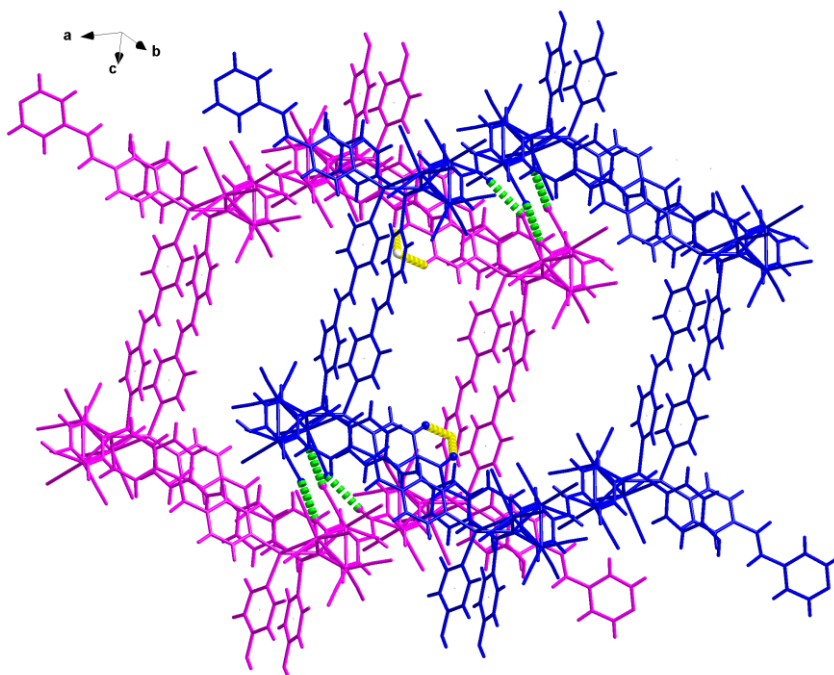
1-bpea-2D



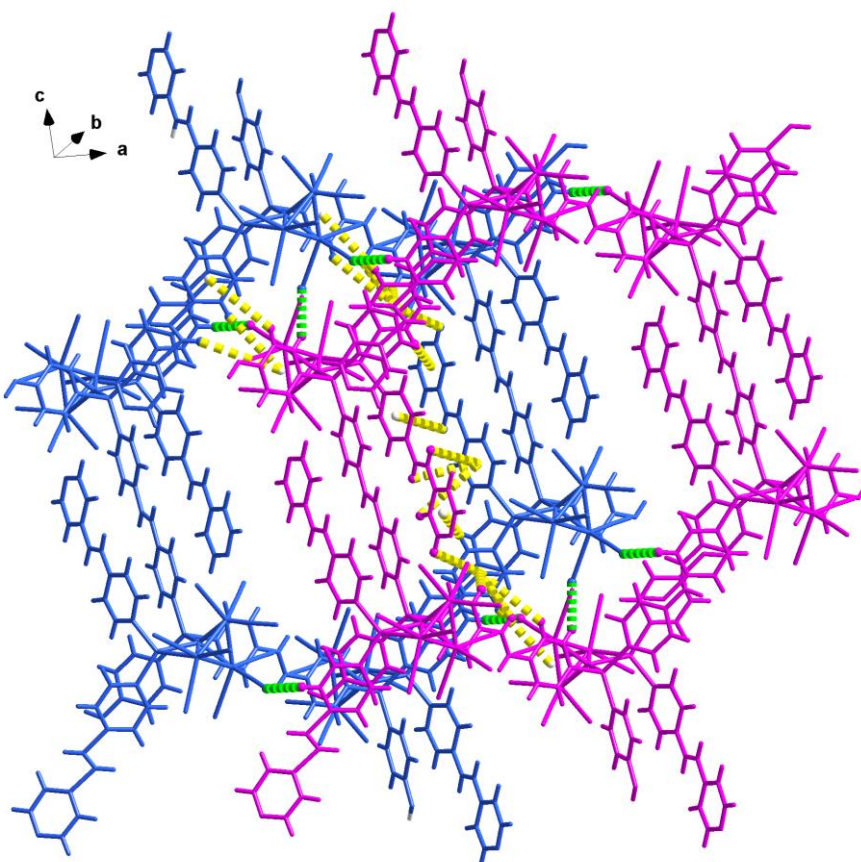
1-bpee-2D-1·MeCN



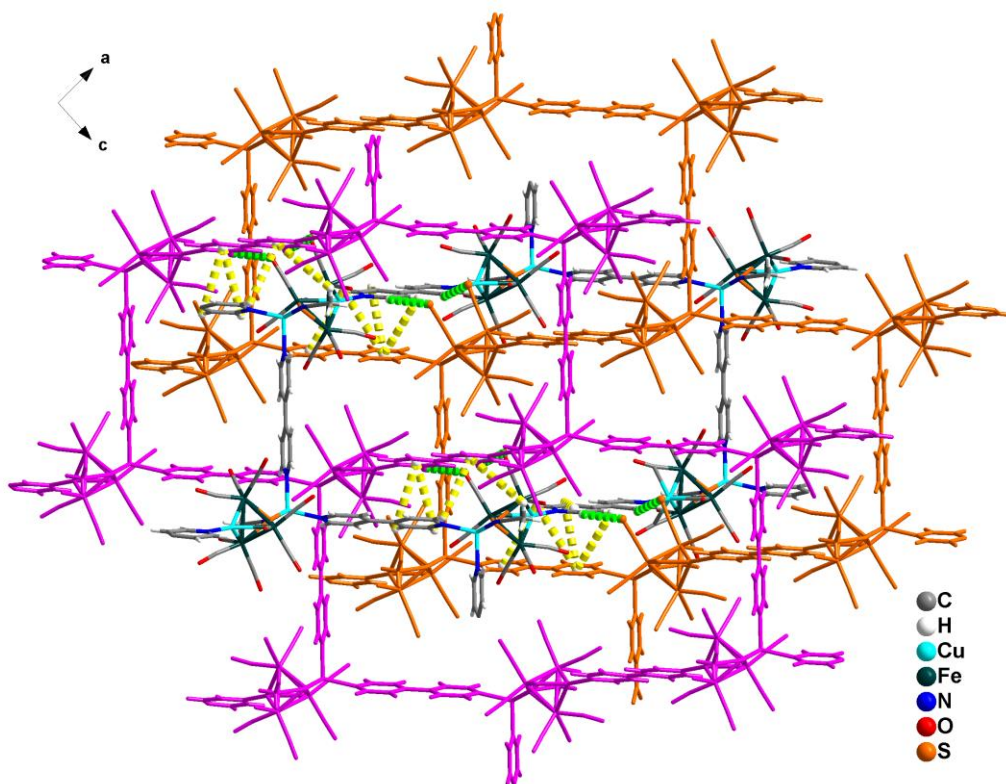
1-bpee-2D-2



1-bpee-2D-3·MeCN (disordered atoms were omitted)



1-dpy-2D



1-dpy-1D

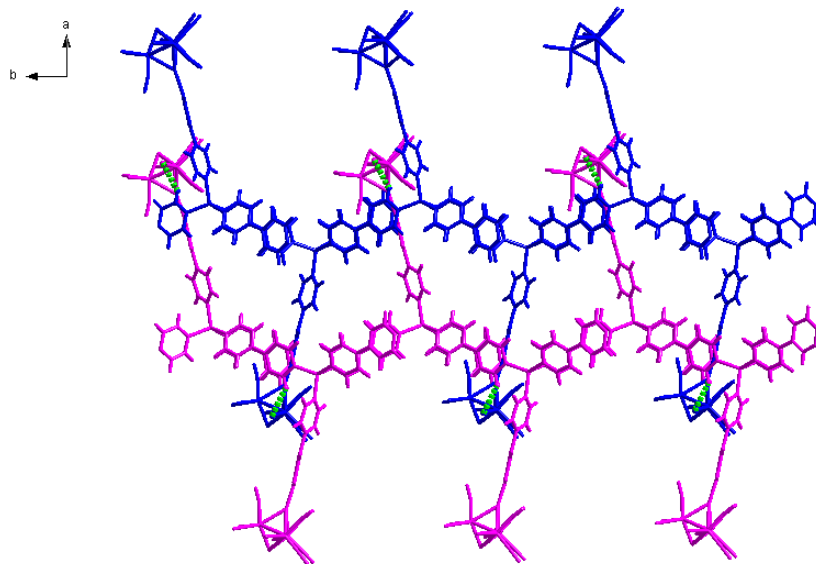
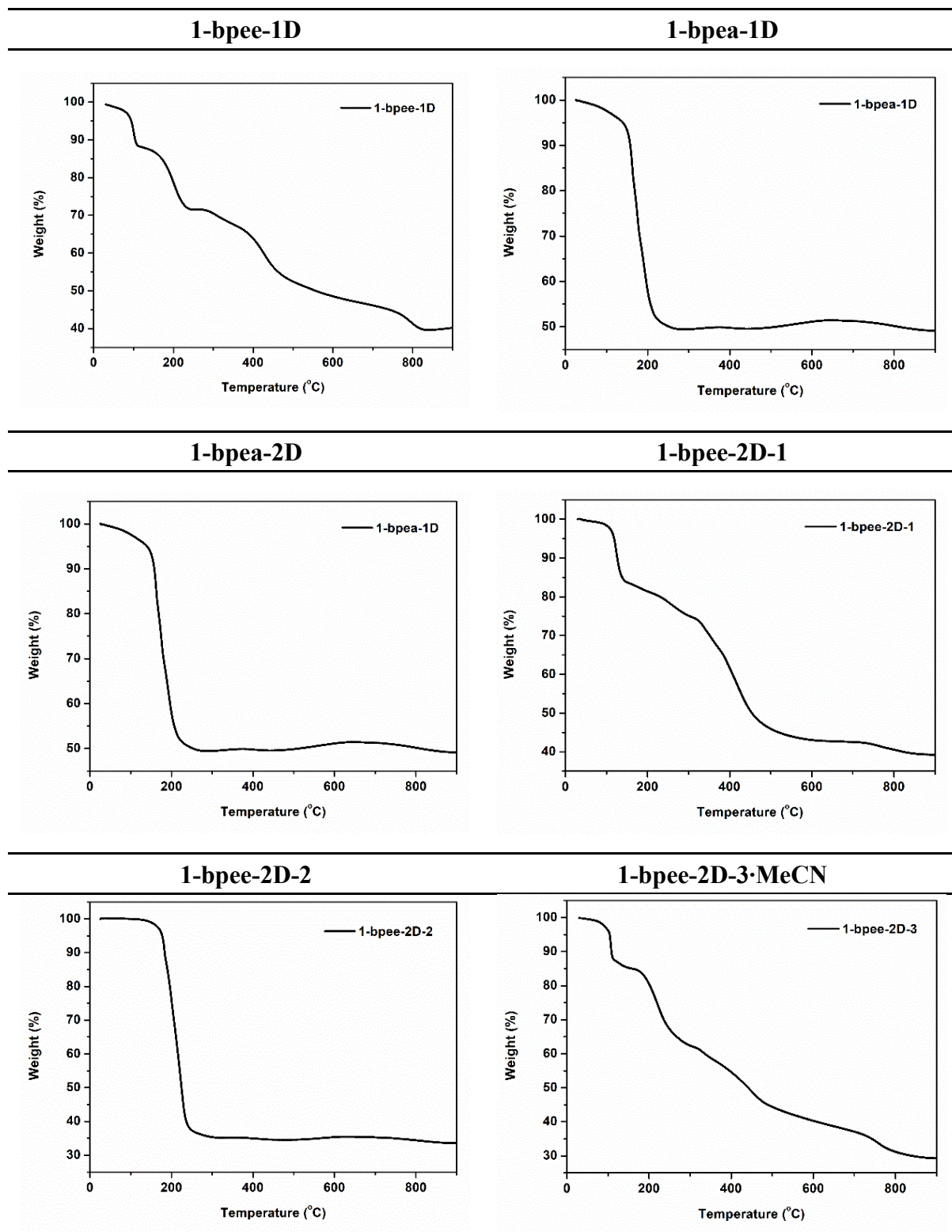
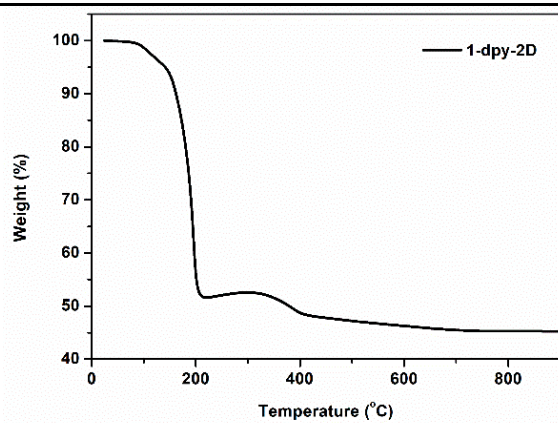


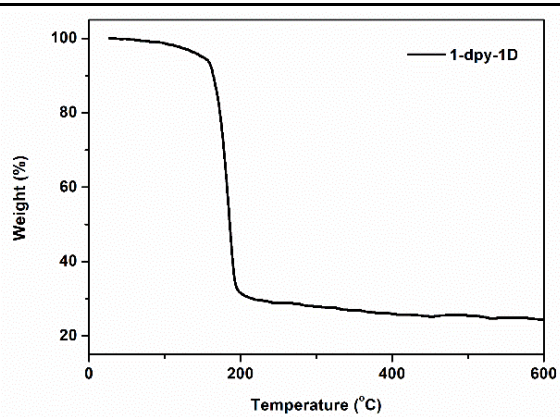
Fig. S12 TGA spectra of all synthesized S–Fe–Cu–CO polymers.



1-dpy-2D



1-dpy-1D



1-bpp-2D

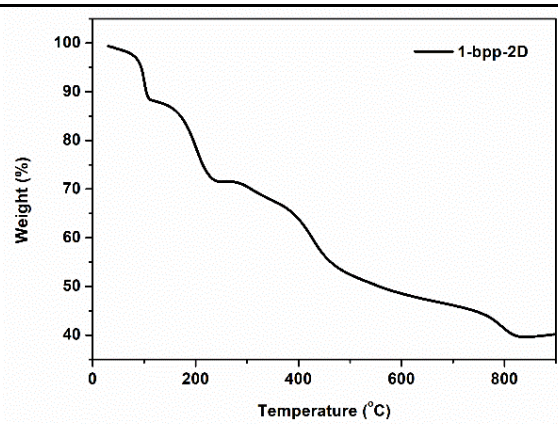
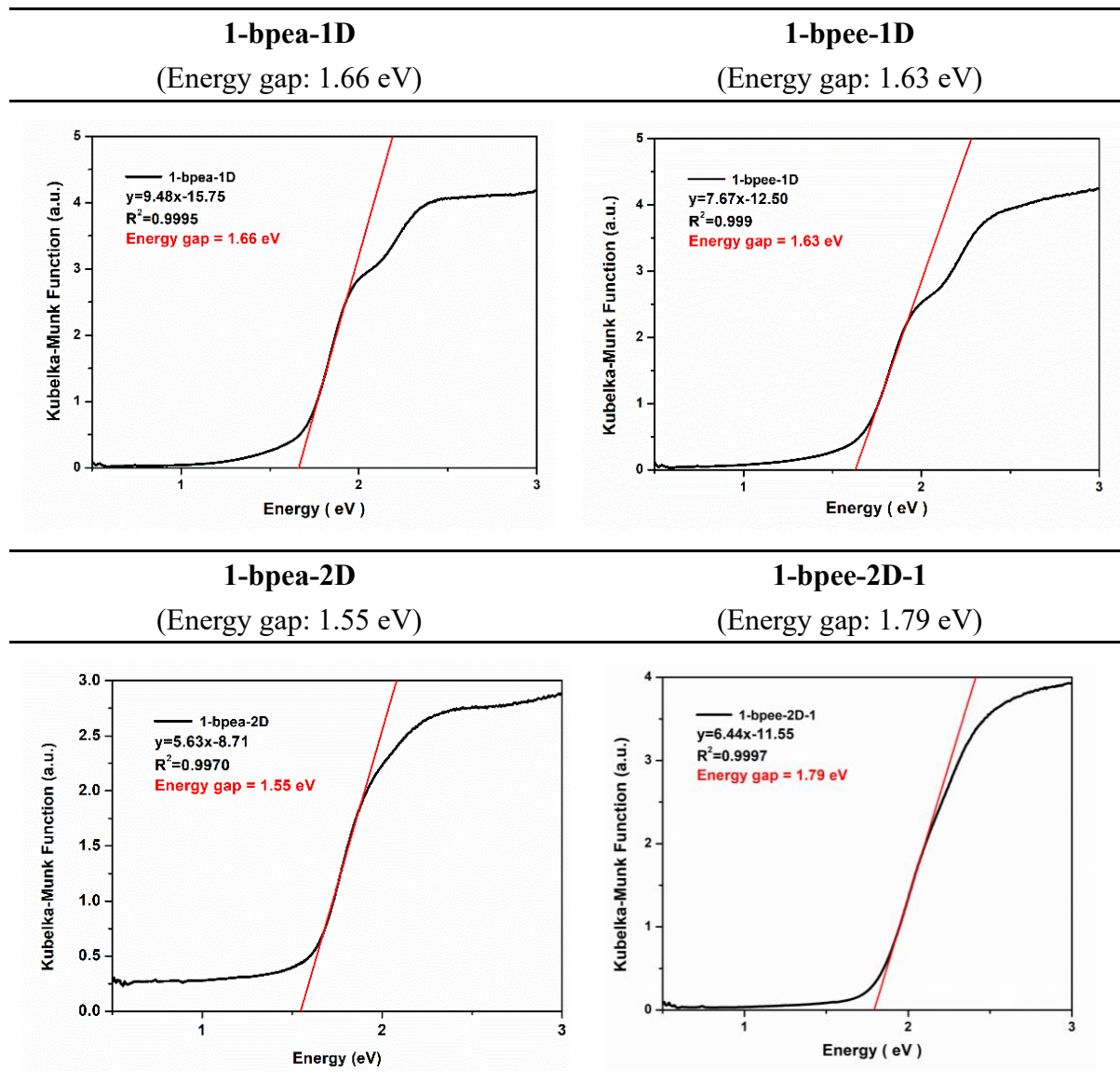
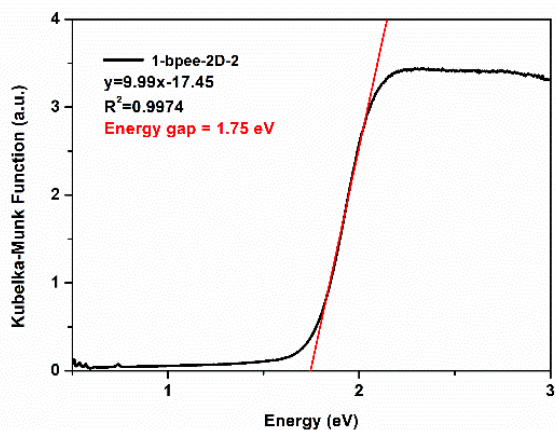


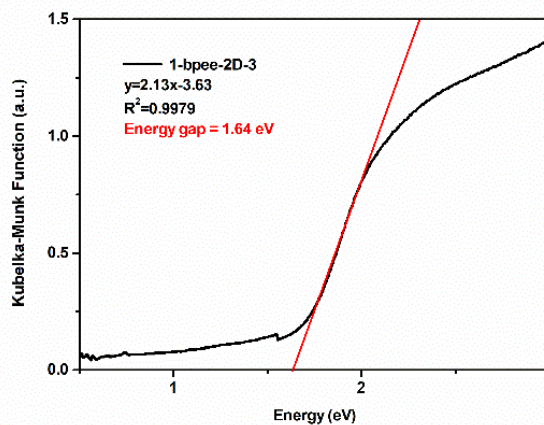
Fig. S13 Diffuse reflectance spectra of all synthesized S–Fe–Cu–CO polymers.



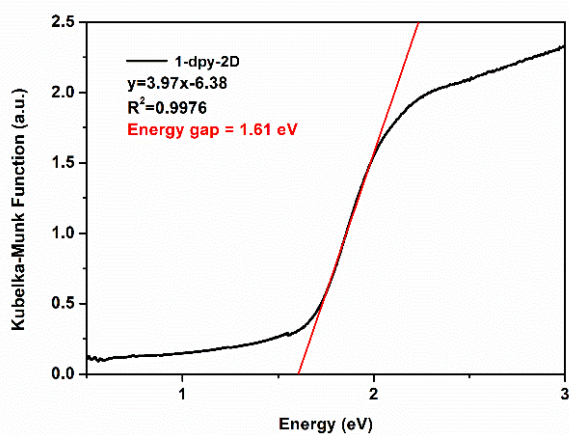
1-bpee-2D-2
(Energy gap: 1.75 eV)



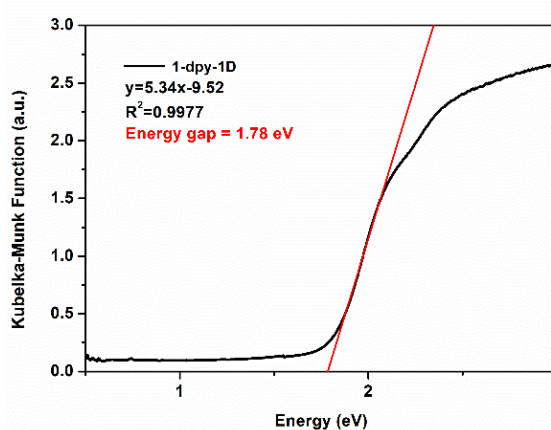
1-bpee-2D-3·MeCN
(Energy gap: 1.64 eV)



1-dpy-2D
(Energy gap: 1.61 eV)



1-dpy-1D
(Energy gap: 1.78 eV)



1-bpp-2D
(Energy gap: 1.58 eV)

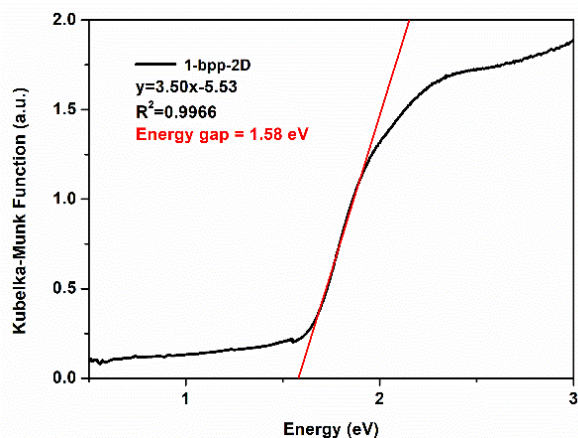
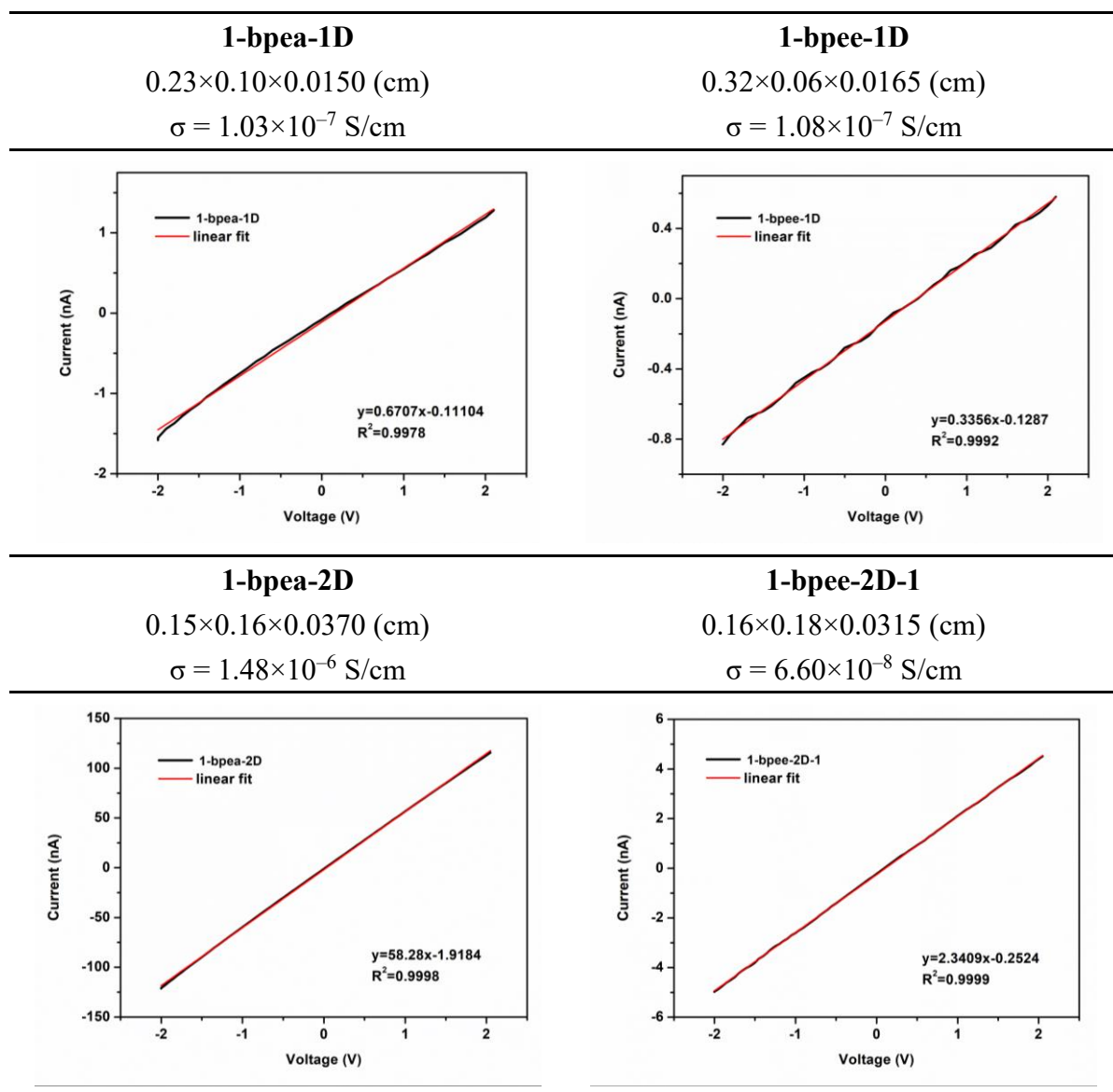


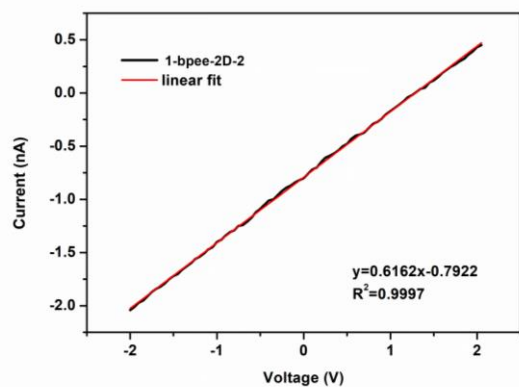
Fig. S14 I - V curves of pressed pellets (length (L) \times width (W) \times thickness (T)) of all synthesized S-Fe-Cu polymers by two-contact probe method at room temperature, in the dark and *vacuo*.



1-bpee-2D-2

0.30×0.18×0.0320 (cm)

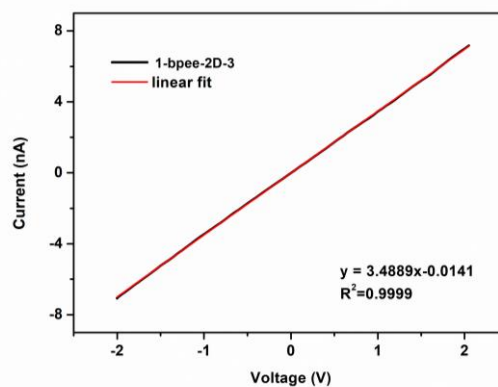
$$\sigma = 3.26 \times 10^{-8} \text{ S/cm}$$



1-bpee-2D-3·MeCN

0.12×0.17×0.0223 (cm)

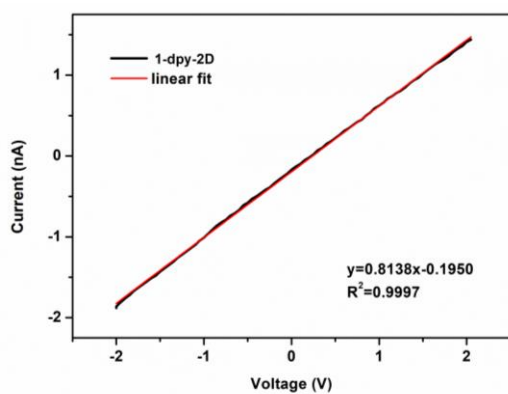
$$\sigma = 1.10 \times 10^{-7} \text{ S/cm}$$



1-dpy-2D

0.40×0.21×0.0148 (cm)

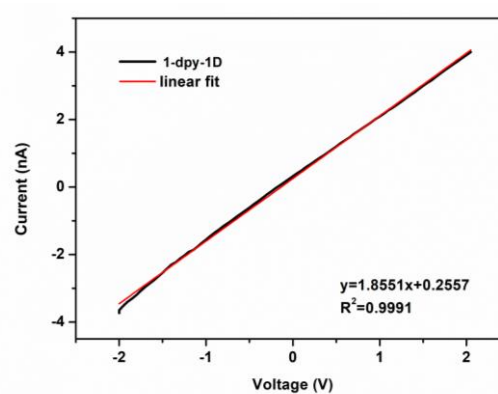
$$\sigma = 1.05 \times 10^{-7} \text{ S/cm}$$



1-dpy-1D

0.23×0.20×0.0265 (cm)

$$\sigma = 8.05 \times 10^{-8} \text{ S/cm}$$



1-bpp-2D

0.22×0.15×0.0370 (cm)

$$\sigma = 4.71 \times 10^{-7} \text{ S/cm}$$

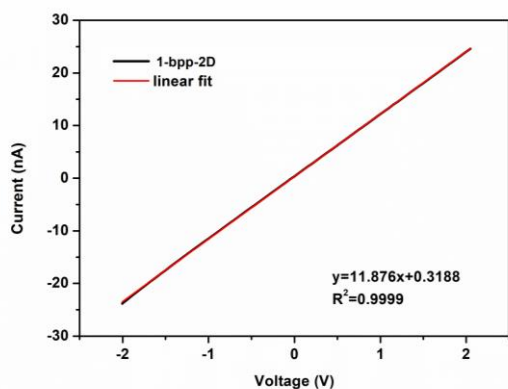
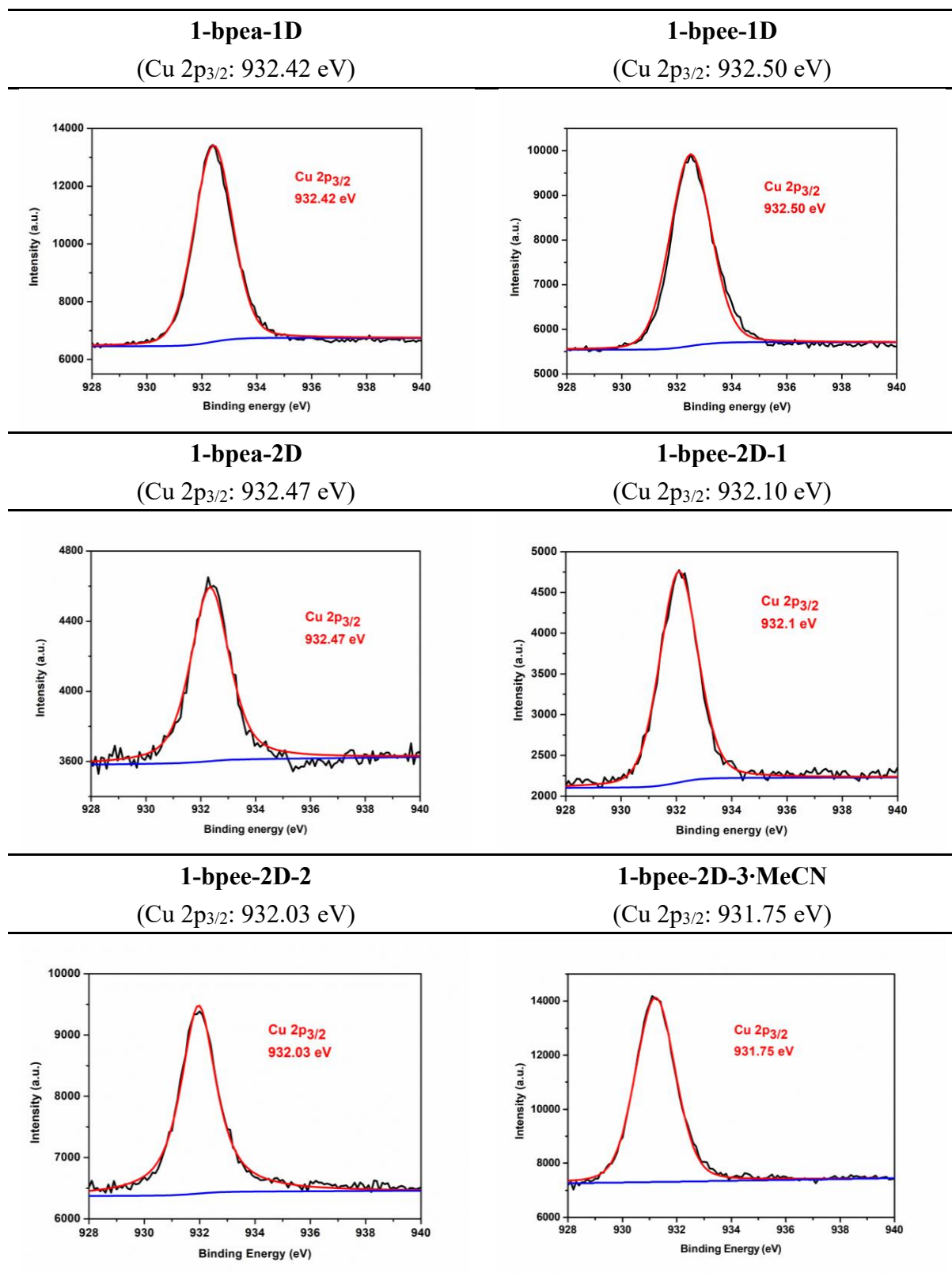
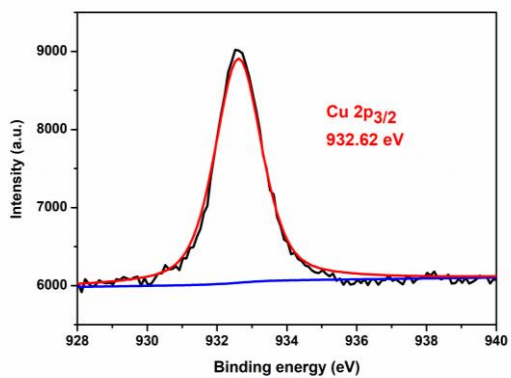


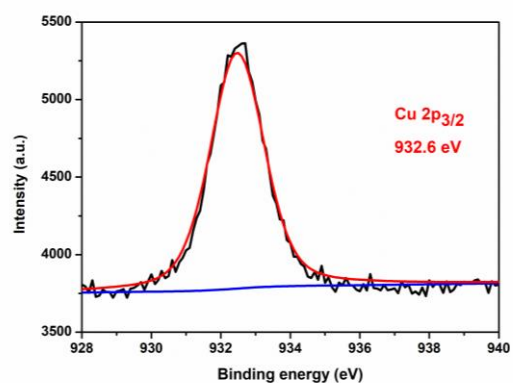
Fig. S15 Experimental (black) and simulated (red) XPS focusing on the Cu 2p_{3/2} region of all synthesized S–Fe–Cu–CO polymers.



1-dpy-2D
(Cu 2p_{3/2}: 932.62 eV)



1-dpy-1D
(Cu 2p_{3/2}: 932.60 eV)



1-bpp-2D
(Cu 2p_{3/2}: 932.50 eV)

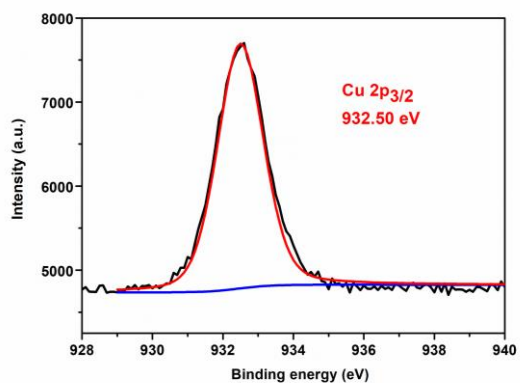
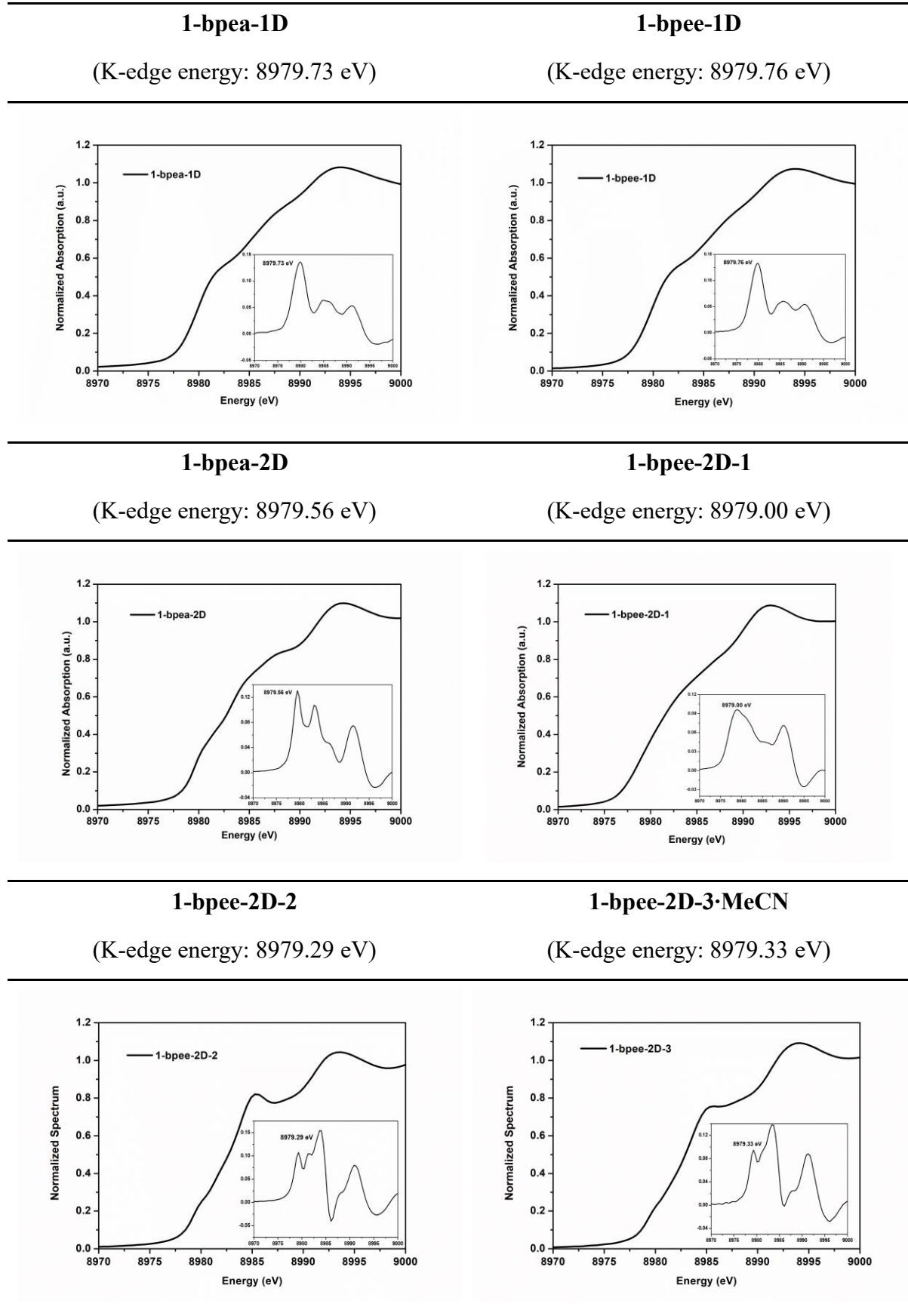
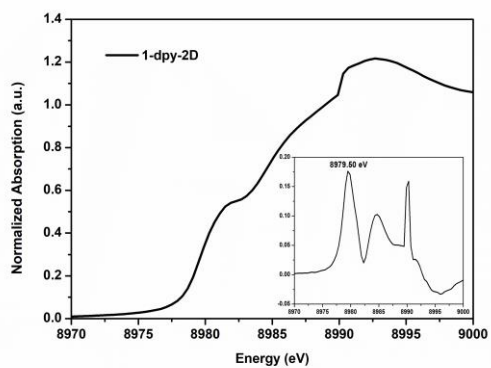


Fig. S16 XANES of all synthesized S–Fe–Cu–CO polymers focusing on Cu K-edge energies.



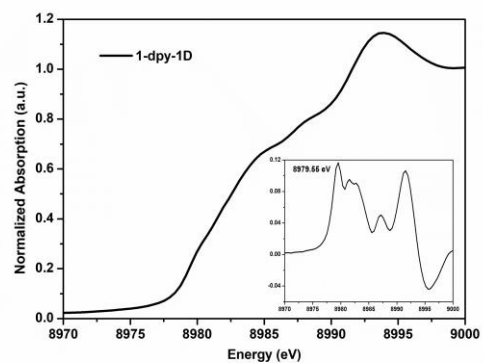
1-dpy-2D

(K-edge energy: 8979.50 eV)



1-dpy-1D

(K-edge energy: 8979.55 eV)



1-bpp-2D

(K-edge energy: 8979.99 eV)

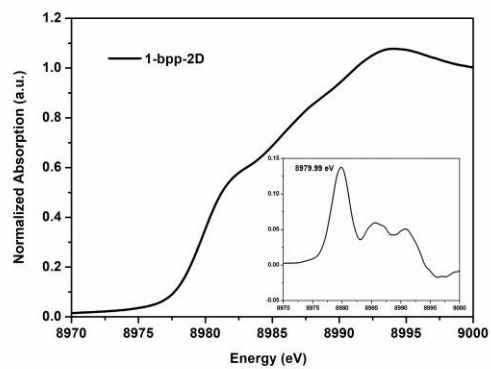
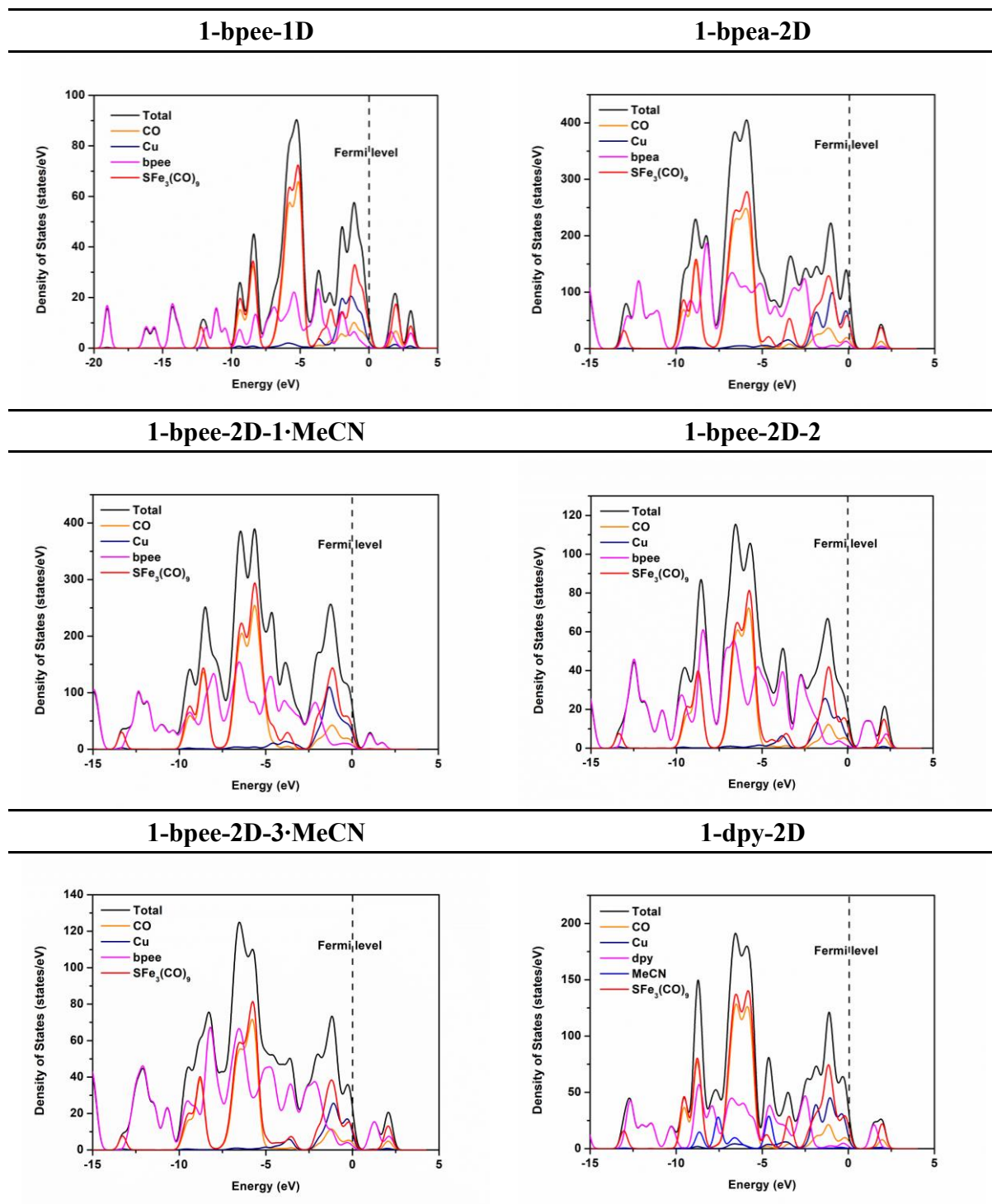
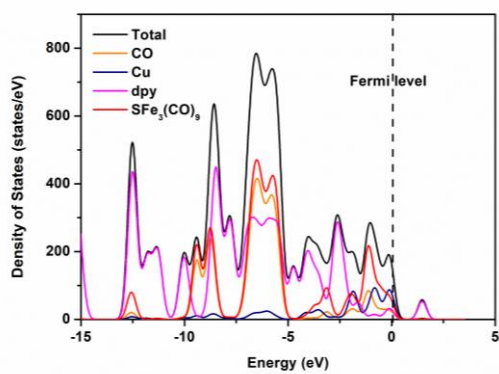


Fig. S17 DOS plots of **1-bpee-1D**, **1-bpea-2D**, **1-bpee-2D-1·MeCN**, **1-bpee-2D-2**, **1-bpee-2D-3·MeCN**, **1-dpy-2D**, **1-dpy-1D**, and **1-bpp-2D**. Total density of states (DOS) (black line) and partial density of states (PDOS) (red line, $\text{SFe}_3(\text{CO})_9$ groups; pink line, dipyriddy ligands; navy line, Cu nodes; orange line, CO; olive line, MeCN) with the Fermi level set as zero.



1-dpy-1D



1-bpp-2D

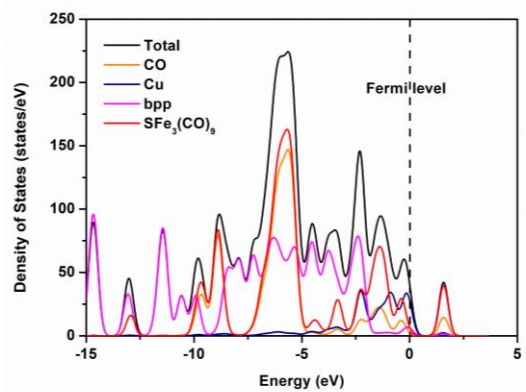
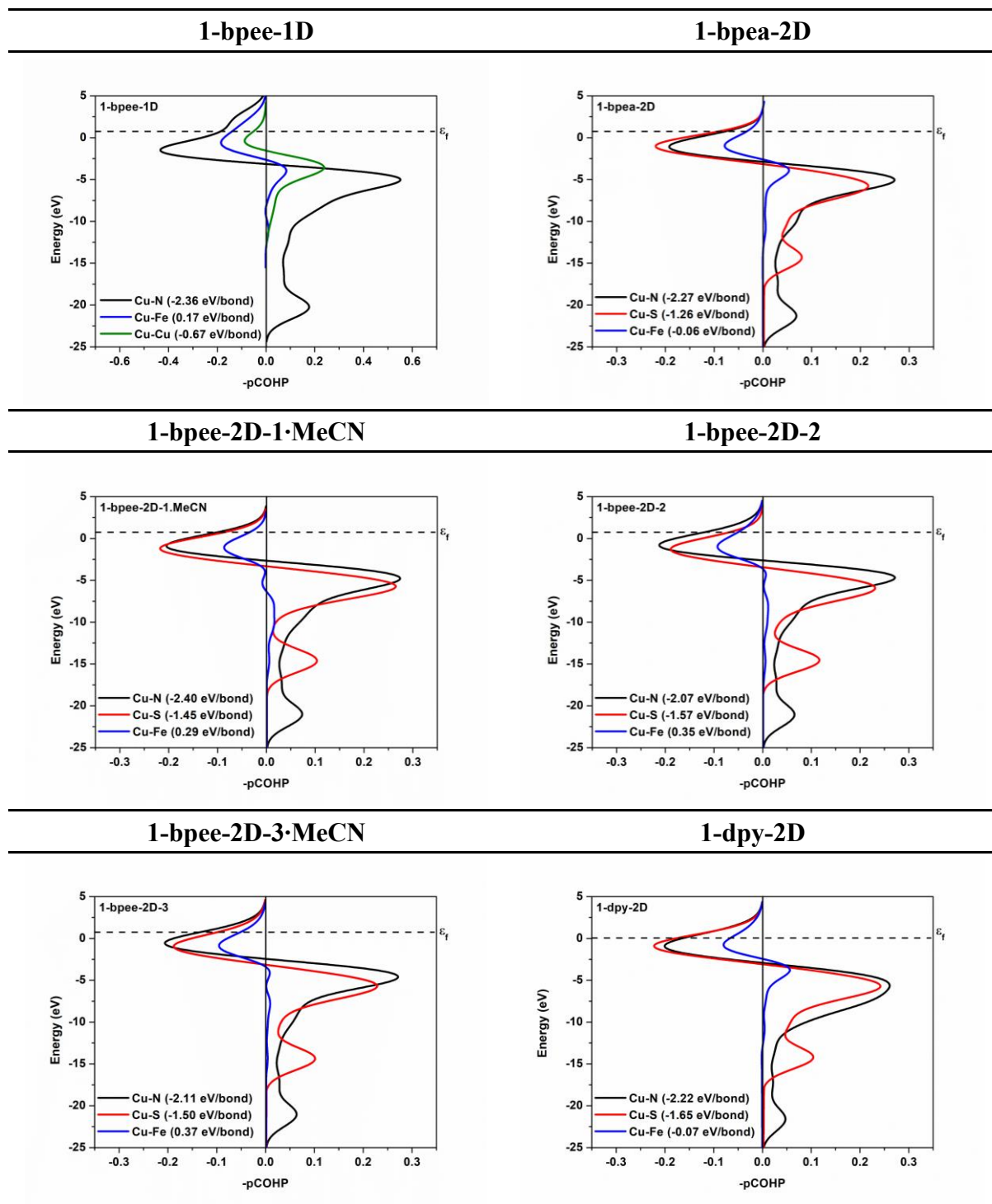
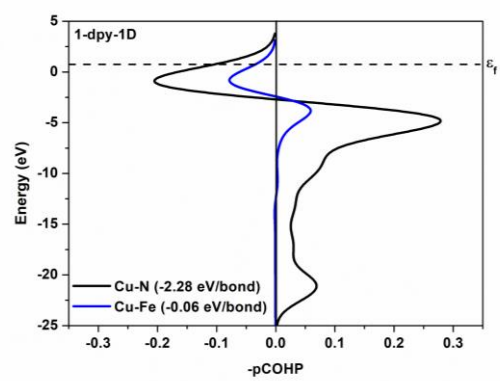


Fig. S18 Projected COHP (pCOHP) plots of selected Cu–N, Cu–S, Cu–Fe, and Cu–Cu bonds in polymers **1-bpee-1D**, **1-bpea-2D**, **1-bpee-2D-1·MeCN**, **1-bpee-2D-2**, **1-bpee-2D-3·MeCN**, **1-dpy-2D**, **1-dpy-1D**, and **1-bpp-2D**. The average integrated pCOHP (ICOHP) values were shown in brackets.



1-dpy-1D



1-bpp-2D

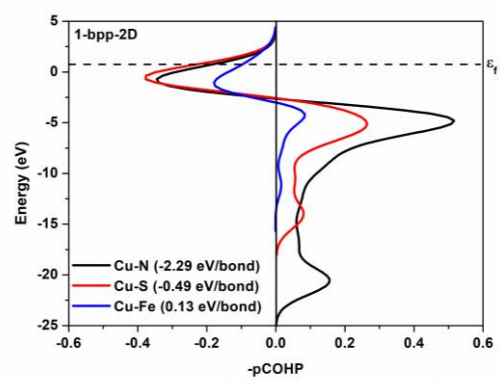
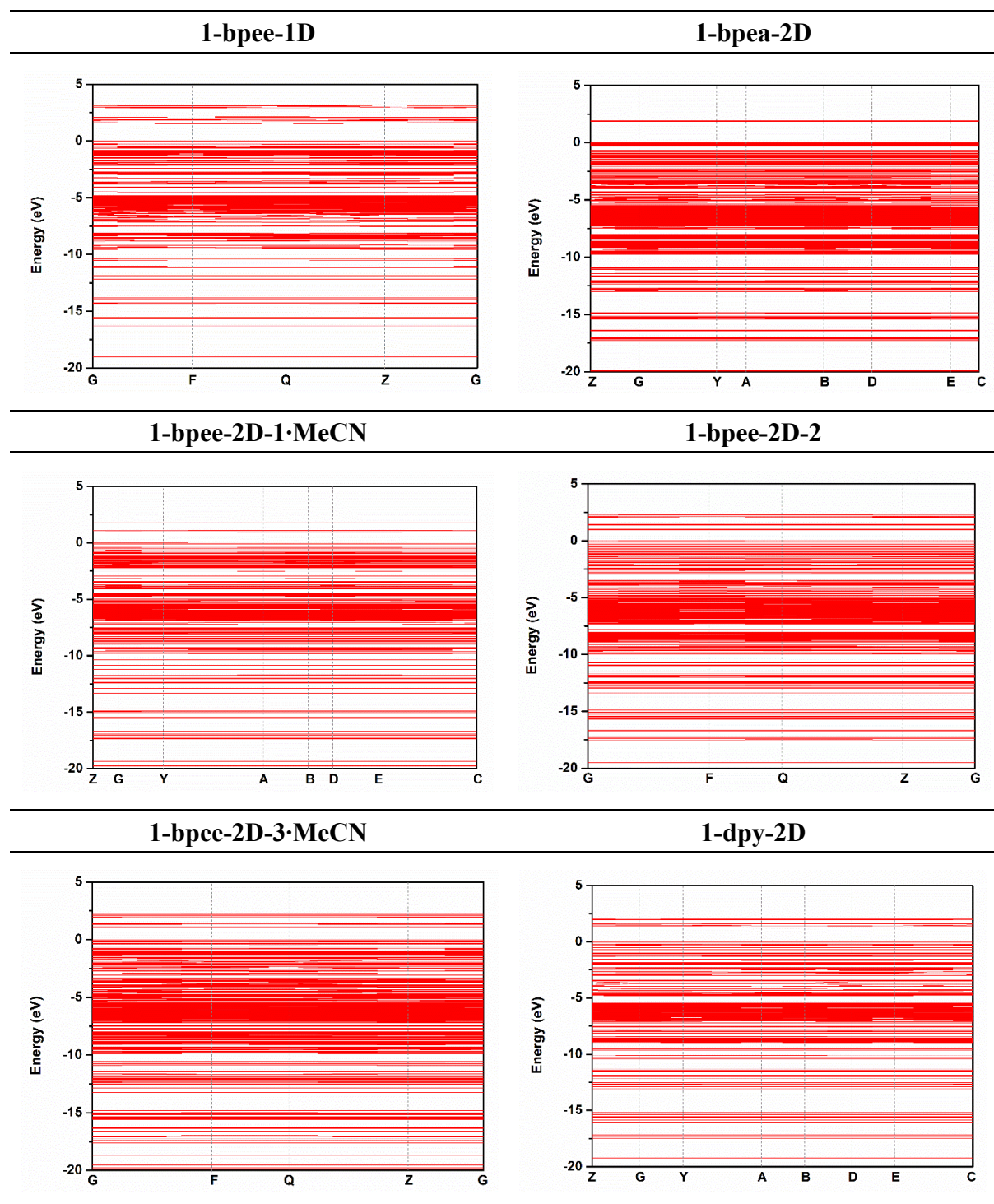
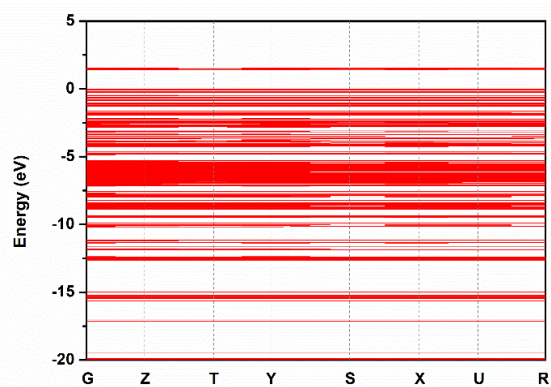


Fig. S19 Calculated band structures of **1-bpee-1D**, **1-bpea-2D**, **1-bpee-2D-1·MeCN**, **1-bpee-2D-2**, **1-bpee-2D-3·MeCN**, **1-dpy-2D**, **1-dpy-1D**, and **1-bpp-2D**, with the Fermi level set as zero.



1-dpy-1D



1-bpp-2D

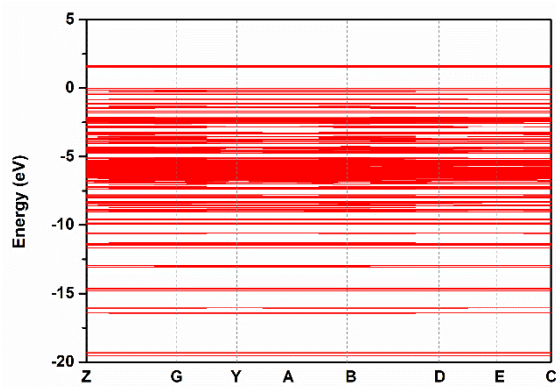


Fig. S20 DPV measurement of **1-bpea-2D**, **1-bpee-1D**, **1-bpee-2D-3·MeCN**, **1-bpee-2D-1**, and **1-dpy-1D** with the corresponding potentials versus a saturated calomel electrode (SCE) are given. Electrolyte, 0.1M Bu₄ClO₄; working electrode, glassy carbon; scan rate, 100mV s⁻¹.

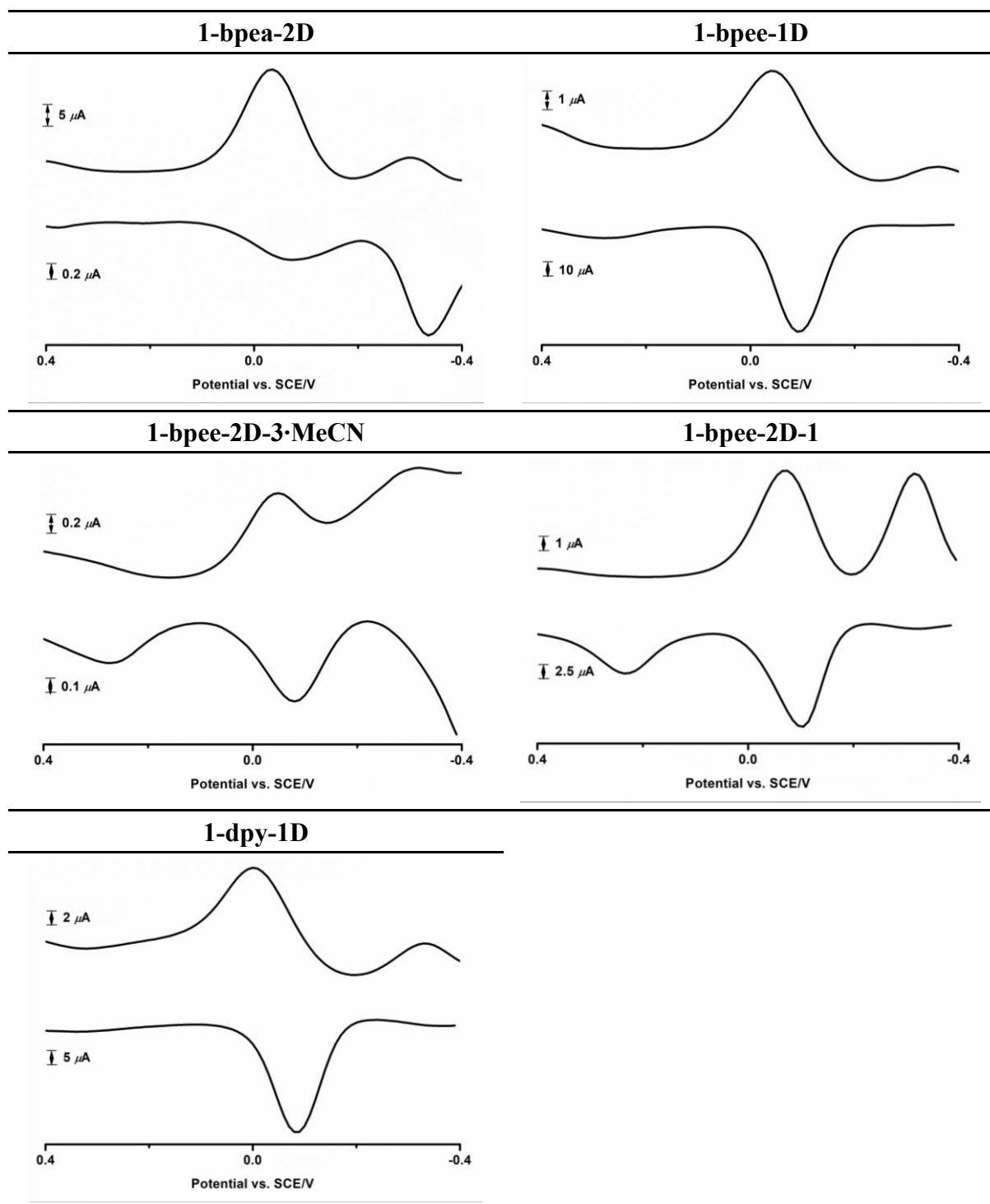


Table S1 Selected crystallographic data for **1-bpea-2D**, **1-bpee-2D-1·MeCN**, **1-bpee-2D-2**, **1-bpee-2D-3·MeCN**, **1-dpy-2D**, and **1-dpy-1D**.

| | 1-bpea-2D | 1-bpee-2D-1·MeCN | 1-bpee-2D-2 |
|---|--|--|--|
| empirical formula | C ₁₃₂ H ₉₆ Cu ₈ Fe ₁₂ N ₁₆ O ₃₆ S ₄ | C ₇₀ H ₄₆ Cu ₄ Fe ₆ N ₁₀ O ₁₈ S ₂ | C ₉₀ H ₆₀ Cu ₄ Fe ₆ N ₁₂ O ₁₈ S ₂ |
| formula weight | 3789.00 | 1968.55 | 2250.88 |
| crystal system | monoclinic | monoclinic | triclinic |
| space group | <i>P</i> 2 ₁ / <i>c</i> | <i>C</i> 2/ <i>c</i> | <i>P</i> $\bar{1}$ |
| crystal dimensions, mm | 0.13 × 0.12 × 0.20 | 0.13 × 0.10 × 0.04 | 0.26 × 0.14 × 0.10 |
| <i>a</i> , Å | 32.1519(9) | 10.1738(6) | 11.7021(4) |
| <i>b</i> , Å | 11.8405(3) | 22.244(1) | 12.1401(4) |
| <i>c</i> , Å | 19.0752(6) | 39.699(2) | 19.7195(7) |
| α , deg | | | 102.299(1) |
| β , deg | 94.033(1) | 91.936(2) | 91.349(1) |
| γ , deg | | | 107.867(1) |
| <i>V</i> , Å ³ | 7243.8(4) | 8979.1(9) | 2593.2(2) |
| <i>Z</i> | 2 | 4 | 1 |
| <i>D</i> (calc), g cm ⁻³ | | 1.456 | 1.441 |
| μ , mm ⁻¹ | 2.444 | 1.975 | 1.721 |
| color, habit | black, prism | black, prism | Brown, prism |
| diffractometer | D8 Venture | D8 Venture | D8 Venture |
| radiation (λ), Å | 0.71073 | 0.71073 | 0.71073 |
| temperature, K | 200(2) | 200(2) | 200(2) |
| θ range for data collection, deg | 2.275/25.036 | 2.202/22.546 | 2.267/25.076 |
| <i>T</i> _{min} / <i>T</i> _{max} | 0.742/0.953 | 0.783/0.925 | 0.663/0.847 |
| no. of independent reflections (<i>I</i> > 2 σ (<i>I</i>)) | 10461 (R _{int} = 0.0593) | 4516 (R _{int} = 0.1046) | 7909 (R _{int} = 0.0404) |
| no. of parameters | 961 | 528 | 589 |
| goodness of fit | 1.029 | 1.074 | 1.041 |
| R1 ^a /wR2 ^a (<i>I</i> > 2 σ (<i>I</i>)) | 0.0395/0.0898 | 0.0707/0.1759 | 0.0299/0.0658 |
| R1 ^a /wR2 ^a (all data) | 0.0548/0.0992 | 0.1400/0.2136 | 0.0385/0.0697 |

| | 1-bpee-2D-3·MeCN | 1-dpy-2D | 1-dpy-1D |
|---|---|---|--|
| empirical formula | C ₁₀₆ H ₇₆ Cu ₄ Fe ₆ N ₁₆ O ₁₈ S ₂ | C ₅₂ H ₃₀ Cu ₄ Fe ₆ N ₈ O ₁₈ S ₂ | C ₇₈ H ₄₈ Cu ₄ Fe ₆ N ₁₂ O ₁₈ S ₂ |
| formula weight | 2515.20 | 1708.22 | 2094.66 |
| crystal system | triclinic | monoclinic | orthorhombic |
| space group | <i>P</i> $\bar{1}$ | <i>P</i> 2 ₁ / <i>n</i> | <i>Pcab</i> |
| crystal dimensions, mm | 0.20 × 0.07 × 0.03 | 0.21 × 0.15 × 0.08 | 0.30 × 0.25 × 0.08 |
| <i>a</i> , Å | 12.1657(5) | 9.9853(8) | 19.8904(3) |
| <i>b</i> , Å | 12.5737(5) | 18.375(1) | 17.0117(3) |
| <i>c</i> , Å | 18.2632(8) | 16.701(1) | 23.7088(3) |
| α , deg | 87.707(1) | | |
| β , deg | 85.287(1) | 92.858(4) | |
| γ , deg | 69.397(1) | | |
| <i>V</i> , Å ³ | 2606.0(2) | 3060.4(4) | 8022.3(2) |
| <i>Z</i> | 1 | 2 | 4 |
| <i>D</i> (calc), g cm ⁻³ | 1.603 | 1.854 | 1.734 |
| μ , mm ⁻¹ | 1.723 | 2.881 | 2.217 |
| color, habit | brown (dark), prism | black, prism | black, prism |
| diffractometer | D8 Venture | Bruker APEX2 | Bruker APEX2 |
| radiation (λ), Å | 0.71073 | 0.71073 | 0.71073 |
| temperature, K | 200(2) | 296(2) | 200(2) |
| θ range for data collection, deg | 2.23/24.99 | 2.217/24.792 | 2.331/24.794 |
| <i>T</i> _{min} / <i>T</i> _{max} | 0.794/0.950 | 0.583/0.802 | 0.556/0.843 |
| no. of independent reflections (<i>I</i> > 2 σ (<i>I</i>)) | 7224 (R _{int} = 0.0466) | 4102 (R _{int} = 0.0307) | 5242 (R _{int} = 0.0519) |
| no. of parameters | 694 | 401 | 541 |
| goodness of fit | 1.174 | 1.146 | 1.014 |
| R1 ^a /wR2 ^a (<i>I</i> > 2 σ (<i>I</i>)) | 0.0320/0.0664 | 0.0343/0.0845 | 0.0299/0.0639 |
| R1 ^a /wR2 ^a (all data) | 0.0543/0.0812 | 0.0551/0.1029 | 0.0511/0.0714 |

^a The functions minimized during least-squares cycles were $R_1 = \Sigma||F_o| - |F_c|| / \Sigma|F_o|$ and $wR_2 = \{\Sigma[w(F_o^2 - F_c^2)^2] / \Sigma[w(F_o^2)]\}^{1/2}$.

Table S2 Selected bond distances (Å) and bond angles (deg) for **1-bpea-2D**, **1-bpee-2D-1-MeCN**, **1-bpee-2D-2**, **1-bpee-2D-3-MeCN**, **1-dpy-2D**, and **1-dpy-1D**.

| 1-bpea-2D | | | |
|---------------------|-----------|----------------------|-----------|
| Cu(1)–Fe(1) | 2.5278(8) | Fe(3)–S(1) | 2.202(1) |
| Cu(1)–Fe(2) | 2.5364(9) | Fe(1')–S(1) | 2.113(6) |
| Cu(1)–Fe(1') | 2.548(6) | Fe(1')–Fe(3') | 2.639(8) |
| Cu(1)–Fe(3) | 2.5527(9) | Fe(1')–Fe(2') | 2.664(8) |
| Cu(1)–Fe(3') | 2.576(6) | Fe(2')–S(1) | 2.232(6) |
| Cu(1)–Fe(2') | 2.610(6) | Fe(2')–Fe(3') | 2.637(8) |
| Cu(2)–S(1) | 2.343 (1) | Fe(3')–S(1) | 2.155(6) |
| Cu(3)–S(2) | 2.282(1) | Fe(4)–S(2) | 2.195(1) |
| Cu(4)–Fe(5) | 2.468(8) | Fe(4)–Fe(6) | 2.6356(8) |
| Cu(4)–Fe(6) | 2.5362(8) | Fe(4)–Fe(5) | 2.6579(8) |
| Cu(4)–Fe(4) | 2.6072(8) | Fe(5)–S(2) | 2.183(1) |
| Fe(1)–S(1) | 2.193(1) | Fe(5)–Fe(6) | 2.6542(8) |
| Fe(1)–Fe(2) | 2.6371(9) | Fe(6)–S(2) | 2.193(1) |
| Fe(1)–Fe(3) | 2.6418(9) | S(1)–Cu(2) | 2.344(1) |
| Fe(2)–S(1) | 2.183(1) | S(2)–Cu(3) | 2.282(1) |
| Fe(2)–Fe(3) | 2.6309(9) | | |
| Fe(1)–Cu(1)–Fe(2) | 62.76(2) | S(1)–Fe(3')–Fe(2') | 54.4(2) |
| Fe(1)–Cu(1)–Fe(3) | 62.66(2) | Cu(1)–Fe(3')–Fe(2') | 60.1(2) |
| Fe(2)–Cu(1)–Fe(3) | 62.26(2) | S(1)–Fe(3')–Fe(1') | 51.1 (2) |
| Fe(1')–Cu(1)–Fe(3') | 62.0(2) | Cu(1)–Fe(3')–Fe(1') | 58.5(2) |
| Fe(1')–Cu(1)–Fe(2') | 62.2(2) | Fe(2')–Fe(3')–Fe(1') | 60.7(2) |
| Fe(3')–Cu(1)–Fe(2') | 61.1(2) | S(2)–Fe(4)–Cu(4) | 96.36(4) |
| Fe(5)–Cu(4)–Fe(6) | 64.05(2) | S(2)–Fe(4)–Fe(6) | 53.04(3) |
| Fe(5)–Cu(4)–Fe(4) | 63.10(2) | Cu(4)–Fe(4)–Fe(6) | 57.86(2) |
| Fe(6)–Cu(4)–Fe(4) | 61.63(2) | S(2)–Fe(4)–Fe(5) | 52.40(3) |
| S(1)–Fe(1)–Cu(1) | 99.52(4) | Cu(4)–Fe(4)–Fe(5) | 55.89(2) |
| S(1)–Fe(1)–Fe(2) | 52.76(3) | Fe(6)–Fe(4)–Fe(5) | 60.19(2) |
| Cu(1)–Fe(1)–Fe(2) | 58.78(2) | S2(1)–Fe(5)–Cu(4) | 100.88(4) |
| S(1)–Fe(1)–Fe(3) | 53.22(3) | S(2)–Fe(5)–Fe(6) | 52.82(3) |
| Cu(1)–Fe(1)–Fe(3) | 59.13(2) | Cu(4)–Fe(5)–Fe(6) | 59.23(2) |
| Fe(2)–Fe(1)–Fe(3) | 59.78(3) | S(2)–Fe(5)–Fe(4) | 52.84(3) |
| S(1)–Fe(2)–Cu(1) | 99.54(4) | Cu(4)–Fe(5)–Fe(4) | 61.02(2) |
| S(1)–Fe(2)–Fe(3) | 53.48(3) | Fe(6)–Fe(5)–Fe(4) | 59.49(2) |
| Cu(1)–Fe(2)–Fe(3) | 59.18(2) | S(2)–Fe(6)–Cu(4) | 98.51(4) |

| | | | |
|----------------------|----------|--------------------|-----------|
| S(1)–Fe(2)–Fe(1) | 53.12(3) | S(2)–Fe(6)–Fe(4) | 53.13(3) |
| Cu(1)–Fe(2)–Fe(1) | 58.46(2) | S(2)–Fe(6)–Fe(5) | 52.48(3) |
| Fe(3)–Fe(2)–Fe(1) | 60.20(2) | Cu(4)–Fe(6)–Fe(5) | 56.72(2) |
| S(1)–Fe(3)–Cu(1) | 98.52(4) | Fe(4)–Fe(6)–Fe(5) | 60.32(2) |
| S(1)–Fe(3)–Fe(2) | 52.79(3) | Fe(1')–S(1)–Fe(3') | 76.4(2) |
| Cu(1)–Fe(3)–Fe(2) | 58.57(2) | Fe(2)–S(1)–Fe(1) | 74.12(4) |
| S(1)–Fe(3)–Fe(1) | 52.89(3) | Fe(2)–S(1)–Fe(3) | 73.73(4) |
| Cu(1)–Fe(3)–Fe(1) | 58.21(2) | Fe(1)–S(1)–Fe(3) | 73.89(4) |
| Fe(2)–Fe(3)–Fe(1) | 60.02(3) | Fe(1')–S(1)–Fe(2') | 75.6(2) |
| S(1)–Fe(1')–Cu(1) | 101.1(2) | Fe(3')–S(1)–Fe(2') | 73.9(2) |
| S(1)–Fe(1')–Fe(3') | 52.5 (2) | Fe(1')–S(1)–Cu(2) | 130.7(2) |
| Cu(1)–Fe(1')–Fe(3') | 59.5 (2) | Fe(3')–S(1)–Cu(2) | 141.2(2) |
| S(1)–Fe(1')–Fe(2') | 54.2 (2) | Fe(2)–S(1)–Cu(2) | 139.51(5) |
| Cu(1)–Fe(1')–Fe(2') | 60.1(2) | Fe(1)–S(1)–Cu(2) | 129.87(5) |
| Fe(3')–Fe(1')–Fe(2') | 59.6(2) | Fe(3)–S(1)–Cu(3) | 138.21(5) |
| S(1)–Fe(2')–Cu(1) | 96.1(2) | Fe(2')–S(1)–Cu(2) | 133.2(2) |
| S(1)–Fe(2')–Fe(3') | 51.7(2) | Fe(5)–S(2)–Fe(6) | 74.69(4) |
| Cu(1)–Fe(2')–Fe(3') | 58.8(2) | Fe(5)–S(2)–Fe(4) | 74.76(4) |
| S(1)–Fe(2')–Fe(1') | 50.2(2) | Fe(6)–S(2)–Fe(4) | 73.83(4) |
| Cu(1)–Fe(2')–Fe(1') | 57.8(2) | Fe(5)–S(2)–Cu(3) | 142.96(5) |
| Fe(3')–Fe(2')–Fe(1') | 59.7(2) | Fe(6)–S(2)–Cu(3) | 133.20(5) |
| S(1)–Fe(3')–Cu(1) | 99.1(2) | Fe(4)–S(2)–Cu(3) | 130.09(5) |

1-bpee-2D-1·MeCN

| | | | |
|-------------------|-----------|-------------------|-----------|
| Cu(1)–S(1) | 2.246(3) | Fe(1)–Fe(2) | 2.593(2) |
| Cu(1)–Fe(1) | 2.614(2) | Fe(1)–Fe(3) | 2.602 (2) |
| Cu(2)–S(1) | 2.335(3) | Fe(2)–S(1) | 2.220(3) |
| Cu(2)–Fe(2) | 2.589(2) | Fe(2)–Fe(3) | 2.596(2) |
| Fe(1)–S(1) | 2.240(3) | Fe(3)–S(1) | 2.184(2) |
| S(1)–Cu(1)–Fe(1) | 54.25(6) | S(1)–Fe(3)–Fe(2) | 54.53(7) |
| S(1)–Cu(2)–Fe(2) | 53.30(7) | S(1)–Fe(3)–Fe(1) | 54.97(7) |
| S(1)–Fe(1)–Fe(2) | 54.10(7) | Fe(2)–Fe(3)–Fe(1) | 59.84(5) |
| S(1)–Fe(1)–Fe(3) | 52.97(6) | Fe(3)–S(1)–Fe(2) | 72.23(8) |
| Fe(2)–Fe(1)–Fe(3) | 59.96(5) | Fe(3)–S(1)–Fe(1) | 72.06(8) |
| S(1)–Fe(1)–Cu(1) | 54.46(6) | Fe(2)–S(1)–Fe(1) | 71.09(8) |
| Fe(2)–Fe(1)–Cu(1) | 103.99(6) | Fe(3)–S(1)–Cu(1) | 119. 6(1) |
| Fe(3)–Fe(1)–Cu(1) | 94.41(5) | Fe(2)–S(1)–Cu(1) | 133.5(1) |

| | | | |
|-------------------|-----------|------------------|----------|
| S(1)–Fe(2)–Cu(2) | 57.48(7) | Fe(1)–S(1)–Cu(1) | 71.29(8) |
| S(1)–Fe(2)–Fe(1) | 54.81(7) | Fe(3)–S(1)–Cu(2) | 131.1(1) |
| Cu(2)–Fe(2)–Fe(1) | 99.81(6) | Fe(2)–S(1)–Cu(2) | 69.23(8) |
| S(1)–Fe(2)–Fe(3) | 53.24(7) | Fe(1)–S(1)–Cu(2) | 120.1(1) |
| Cu(2)–Fe(2)–Fe(3) | 104.99(6) | Cu(1)–S(2)–Cu(2) | 108.8(1) |
| Fe(1)–Fe(2)–Fe(3) | 60.20(5) | | |

1-bpee-2D-2

| | | | |
|-------------------|-----------|-------------------|-----------|
| Cu(1)–S(1) | 2.2697(7) | Fe(1)–Fe(2) | 2.5986(5) |
| Cu(2)–S(1) | 2.2785(7) | Fe(2)–S(1) | 2.2462(7) |
| Cu(2)–Fe(2) | 2.5764(5) | Fe(2)–Fe(3) | 2.6057(5) |
| Fe(1)–S(1) | 2.1938(7) | Fe(3)–S(1) | 2.1893(7) |
| Fe(1)–Fe(3) | 2.5861(5) | | |
| S(1)–Cu(2)–Fe(2) | 54.70(2) | Fe(1)–Fe(3)–Fe(2) | 60.07(1) |
| S(1)–Fe(1)–Fe(3) | 53.76(2) | Fe(1)–S(1)–Fe(1) | 72.32(2) |
| S(1)–Fe(1)–Fe(2) | 55.12(2) | Fe(3)–S(1)–Fe(2) | 71.94(2) |
| Fe(3)–Fe(1)–Fe(2) | 60.34(1) | Fe(1)–S(1)–Fe(2) | 71.63(2) |
| S(1)–Fe(2)–Cu(2) | 55.89(2) | Fe(3)–S(1)–Cu(1) | 133.66(3) |
| S(1)–Fe(2)–Fe(1) | 53.25(2) | Fe(1)–S(1)–Cu(1) | 119.12(3) |
| Cu(2)–Fe(2)–Fe(1) | 103.45(2) | Fe(2)–S(1)–Cu(1) | 153.16(3) |
| S(1)–Fe(2)–Fe(3) | 53.02(2) | Fe(3)–S(1)–Cu(2) | 120.81(3) |
| Cu(2)–Fe(2)–Fe(3) | 97.14(2) | Fe(1)–S(1)–Cu(2) | 130.56(3) |
| Fe(1)–Fe(2)–Fe(3) | 59.59(1) | Fe(2)–S(1)–Cu(2) | 69.41(2) |
| S(1)–Fe(3)–Fe(1) | 53.92(2) | Cu(1)–S(1)–Cu(2) | 87.06(2) |
| S(1)–Fe(3)–Fe(2) | 55.04(2) | | |

1-bpee-2D-3·MeCN

| | | | |
|------------------|-----------|-------------------|-----------|
| S(1)–Fe(2) | 2.1934(9) | Fe(1)–Cu(1) | 2.5791(6) |
| S(1)–Fe(3) | 2.1946(9) | Fe(1)–Fe(2) | 2.5843(6) |
| S(1)–Fe(1) | 2.2622(8) | Fe(1)–Fe(3) | 2.5908(7) |
| S(1)–Cu(2) | 2.2961(8) | Fe(2)–Fe(3) | 2.5841(6) |
| S(1)–Cu(1) | 2.3011(9) | | |
| Fe(2)–S(1)–Fe(3) | 72.16(3) | Cu(1)–Fe(1)–Fe(2) | 100.58(2) |
| Fe(2)–S(1)–Fe(1) | 70.88(3) | S(1)–Fe(1)–Fe(3) | 53.25(2) |
| Fe(3)–S(1)–Fe(1) | 71.07(3) | Cu(1)–Fe(1)–Fe(3) | 101.32(2) |
| Fe(2)–S(1)–Cu(2) | 128.64(4) | Fe(2)–Fe(1)–Fe(3) | 59.92(2) |

| | | | |
|------------------|-----------|-------------------|----------|
| Fe(3)–S(1)–Cu(2) | 121.45(4) | S(1)–Fe(2)–Fe(3) | 53.94(2) |
| Fe(1)–S(1)–Cu(2) | 157.89(4) | S(1)–Fe(2)–Fe(1) | 55.80(2) |
| Fe(2)–S(1)–Cu(1) | 124.18(4) | Fe(3)–Fe(2)–Fe(1) | 60.17(2) |
| Fe(3)–S(1)–Cu(1) | 125.57(4) | S(1)–Fe(3)–Fe(2) | 53.90(2) |
| Fe(1)–S(1)–Cu(1) | 68.82(3) | S(1)–Fe(3)–Fe(1) | 55.68(2) |
| Cu(2)–S(1)–Cu(1) | 89.66(3) | Fe(2)–Fe(3)–Fe(1) | 59.92(2) |
| S(1)–Fe(1)–Cu(1) | 56.30(2) | S(1)–Cu(1)–Fe(1) | 54.87(2) |
| S(1)–Fe(1)–Fe(2) | 53.32(2) | | |

1-dpy-2D

| | | | |
|-------------------|-----------|-------------------|-----------|
| Cu(1)–Fe(1) | 2.5148(7) | Fe(1)–Fe(2) | 2.6443(8) |
| Cu(1)–Fe(2) | 2.5313(8) | Fe(1)–Fe(3) | 2.6729(8) |
| Cu(1)–Fe(3) | 2.5588(7) | Fe(2)–S(1) | 2.188 (1) |
| Cu(2)–S(1) | 2.259(1) | Fe(2)–Fe(3) | 2.638(1) |
| Fe(1)–S(1) | 2.191(1) | Fe(3)–S(1) | 2.182(1) |
| Fe(1)–Cu(1)–Fe(2) | 63.20(2) | Fe(3)–Fe(2)–Fe(1) | 60.80(2) |
| Fe(1)–Cu(1)–Fe(3) | 63.58(2) | S(1)–Fe(3)–Cu(1) | 97.83(4) |
| Fe(2)–Cu(1)–Fe(3) | 62.42(2) | S(1)–Fe(3)–Fe(2) | 52.98(3) |
| S(1)–Fe(1)–Cu(1) | 98.91(3) | Cu(1)–Fe(3)–Fe(2) | 58.28(2) |
| S(1)–Fe(1)–Fe(2) | 52.81(3) | S(1)–Fe(3)–Fe(1) | 52.46(3) |
| Cu(1)–Fe(1)–Fe(2) | 58.70(2) | Cu(1)–Fe(3)–Fe(1) | 57.41(2) |
| S(1)–Fe(1)–Fe(3) | 52.17(3) | Fe(2)–Fe(3)–Fe(1) | 59.72(2) |
| Cu(1)–Fe(1)–Fe(3) | 59.01(2) | Fe(3)–S(1)–Fe(2) | 74.26(4) |
| Fe(2)–Fe(1)–Fe(3) | 59.48(2) | Fe(3)–S(1)–Fe(1) | 75.37(4) |
| S(1)–Fe(2)–Cu(1) | 98.48(4) | Fe(2)–S(1)–Fe(1) | 74.30(4) |
| S(1)–Fe(2)–Fe(3) | 52.76(3) | Fe(3)–S(1)–Cu(2) | 131.12(5) |
| Cu(1)–Fe(2)–Fe(3) | 59.30(2) | Fe(2)–S(1)–Cu(2) | 124.81(5) |
| S(1)–Fe(2)–Fe(1) | 52.89(3) | Fe(1)–S(1)–Cu(2) | 148.22(5) |
| Cu(1)–Fe(2)–Fe(1) | 58.09(2) | | |

1-dpy-1D

| | | | |
|-------------|-----------|-------------|-----------|
| Cu(1)–Fe(1) | 2.4745(5) | Fe(1)–Fe(3) | 2.6779(6) |
| Cu(1)–Fe(3) | 2.5161(5) | Fe(2)–S(1) | 2.1976(8) |
| Cu(1)–Fe(2) | 2.5514(5) | Fe(2)–Fe(3) | 2.6143(5) |
| Fe(1)–S(1) | 2.1759(8) | Fe(3)–S(1) | 2.1923(8) |
| Fe(1)–Fe(2) | 2.6763(6) | | |

| | | | |
|-------------------|----------|-------------------|----------|
| Fe(1)–Cu(1)–Fe(3) | 64.90(2) | S(1)–Fe(2)–Fe(1) | 51.90(2) |
| Fe(1)–Cu(1)–Fe(2) | 64.33(2) | Cu(1)–Fe(2)–Fe(1) | 56.44(1) |
| Fe(3)–Cu(1)–Fe(2) | 62.11(2) | Fe(3)–Fe(2)–Fe(1) | 60.80(2) |
| S(1)–Fe(1)–Cu(1) | 99.38(3) | S(1)–Fe(3)–Cu(1) | 97.68(2) |
| S(1)–Fe(1)–Fe(2) | 52.64(2) | S(1)–Fe(3)–Fe(2) | 53.54(2) |
| Cu(1)–Fe(1)–Fe(2) | 59.23(2) | Cu(1)–Fe(3)–Fe(2) | 59.61(1) |
| S(1)–Fe(1)–Fe(3) | 52.47(2) | S(1)–Fe(3)–Fe(1) | 51.91(2) |
| Cu(1)–Fe(1)–Fe(3) | 58.30(2) | Cu(1)–Fe(3)–Fe(1) | 56.80(2) |
| Fe(2)–Fe(1)–Fe(3) | 58.45(2) | Fe(2)–Fe(3)–Fe(1) | 60.74(2) |
| S(1)–Fe(2)–Cu(1) | 96.52(2) | Fe(1)–S(1)–Fe(3) | 75.62(3) |
| S(1)–Fe(2)–Fe(3) | 53.36(2) | Fe(1)–S(1)–Fe(2) | 75.46(3) |
| Cu(1)–Fe(2)–Fe(3) | 58.28(1) | Fe(3)–S(1)–Fe(2) | 73.10(3) |

Table S3 Detailed investigation of TGA spectra.

| Polymers | Found (%) | Calcd. (%) | Found–Calcd. (%) | Residue | T _{decomp.} (°C) |
|-------------------------|-----------|------------|------------------|---|---------------------------|
| 1-bpea-1D | 50.27 | 50.16 | 0.11 | SFe ₃ Cu ₂ N ₄ | 150 |
| 1-bpee-1D | 48.31 | 48.45 | 0.14 | SFe ₃ Cu ₂ N ₃ | 100 |
| 1-bpea-2D | 35.79 | 35.97 | 0.18 | SFe ₃ Cu ₂ N | 150 |
| 1-bpee-2D-1 | 39.23 | 39.09 | 0.14 | SFe ₃ Cu ₂ N ₃ | 105 |
| 1-bpee-2D-2 | 33.68 | 32.76 | 0.08 | SFe ₃ Cu ₂ N ₃ | 150 |
| 1-bpee-2D-3·MeCN | 29.36 | 29.16 | 0.20 | SFe ₃ Cu ₂ N ₃ | 100 |
| 1-dpy-2D | 45.25 | 44.81 | 0.44 | SFe ₃ Cu ₂ N ₄ | 99 |
| 1-dpy-1D | 31.16 | 31.19 | 0.03 | SFe ₃ Cu ₂ | 94 |
| 1-bpp-2D | 39.69 | 39.24 | 0.45 | SFe ₃ Cu ₂ N ₄ | 100 |

Table S4 Contributions (%) in PDOS for valence and conduction bands of **1-dpy-2D**, **1-bpea-2D**, **1-bpp-2D**, **1-bpee-1D**, **1-bpee-2D-2**, **1-bpee-2D-3·MeCN**, **1-bpee-2D-1·MeCN**, and **1-dpy-1D**.

| Polymers | Bonding Modes | Valence band (VB) (%) | | | | Conduction band (CB) (%) | | | |
|-------------------------|---------------|-----------------------|-------|-------|------------------------------------|--------------------------|----|-------|------------------------------------|
| | | CO | Cu | L | SFe ₃ (CO) ₉ | CO | Cu | L | SFe ₃ (CO) ₉ |
| 1-dpy-2D | L | 16.14 | 41.64 | 3.48 | 54.34 | 17.88 | – | 49.85 | 48.85 |
| 1-bpea-2D | L | 15.87 | 41.67 | 3.99 | 54.01 | 29.71 | – | 10.05 | 87.22 |
| 1-bpp-2D | L | 19.04 | 36.37 | 6.69 | 57.64 | 26.94 | – | 6.84 | 73.27 |
| 1-bpee-1D | B | 16.01 | 36.90 | 13.36 | 50.28 | 31.56 | – | 28.14 | 67.70 |
| 1-bpee-2D-2 | OA | 15.48 | 36.89 | 12.79 | 50.99 | 12.48 | – | 66.87 | 34.05 |
| 1-bpee-2D-3·MeCN | OA | 14.04 | 33.43 | 21.49 | 45.74 | 12.65 | – | 66.04 | 34.50 |
| 1-bpee-2D-1·MeCN | A | 15.48 | 37.48 | 11.96 | 50.16 | – | – | 93.58 | – |
| 1-dpy-1D | P | 21.04 | 31.77 | 13.13 | 55.09 | – | – | 91.86 | – |

References

1. M. Shieh, C.-C. Yu, C.-Y. Miu, C.-H. Kung, C.-Y. Huang, Y.-H. Liu, H.-L. Liu and C.-C. Shen, *Chem. Eur. J.*, 2017, **23**, 11261–11271.
2. Y.-H. Liu, K.-T. Huang, W.-C. Chen, Y.-W. Li, W.-M. Ke, B.-R. Ho, M.-C. Hsu, Y.-H. Li and M. Shieh, *Inorg. Chem.*, 2021, **60**, 18270–18282.
3. G. M. Sheldrick, *SADABS*, Bruker AXS Inc., Madison, Wisconsin, USA, 2003.
4. G. M. Sheldrick, *Acta Cryst.*, 2008, **64**, 112–122.
5. (a) B. Delley, *J. Chem. Phys.*, 1990, **92**, 508–517; (b) B. Delley, *J. Chem. Phys.*, 2000, **113**, 7756–7764.
6. J. P. Perdew, K. Burke and M. Ernzerhof, *Phys. Rev. Lett.*, 1996, **77**, 3865–3868.
7. S. Grimme, *J. Comput. Chem.*, 2004, **25**, 1463–1473.
8. (a) A. Bergner, M. Dolg, W. Küchle, H. Stoll and H. Preuß, *Mol. Phys.*, 1993, **80**, 1431–1441; (b) D. Andrae, U. Haeussermann, M. Dolg, H. Stoll and H. Preuss, *Theor. Chim. Acta*, 1990, **77**, 123–141; (c) P. Schwerdtfeger, M. Dolg, W. E. Schwarz, G. A. Bowmaker and P. D. Boyd, *J. Chem. Phys.*, 1989, **91**, 1762–1774; (d) P. J. Hay and W. R. Wadt, *J. Chem. Phys.*, 1985, **82**, 299–310.
9. (a) P. Kubelka, *Z. Tech. Phys.*, 1931, **12**, 593–601; (b) J. Tauc, *Mater. Res. Bull.*, 1970, **5**, 721–729.
10. B. Ravel and M. Newville, *J. Synchrotron Radiat.*, 2005, **12**, 537–541.
11. A. J. Bard, L. R. Faulkner and H. S. White, *Electrochemical methods: fundamentals and applications*, John Wiley & Sons, 2022.
12. T. Nakanishi, H. Murakami, T. Sagara and N. Nakashima, *J. Phys. Chem. B.*, 1999, **103**, 304–308.